Alignment and Parallelism for the Description of High-Resolution Remote Sensing Images

Maria Carolina Vanegas, Isabelle Bloch, *Member, IEEE*, and Jordi Inglada, *Member, IEEE*

***Abstract*—Alignment and parallelism are frequently found between objects in high-resolution remote sensing images and can be used to interpret and describe the observed scenes. In this paper, we propose new representations of parallelism and alignment as fuzzy spatial relations, which capture the imprecision in the semantics of both relations. We propose two novel definitions of alignment between objects: *local* and *global*. In *local* alignment, each object of the group is aligned with its neighbors, while in *global* alignment, every object of the group is aligned to all other members. Both definitions consider each object as a whole and are based on relative position measures. They are robust with respect to segmentation errors. Furthermore, we propose an efficient graph-based method to determine which are the *locally* and the *globally* aligned groups of objects from a set of segmented objects. In addition, we propose a fuzzy definition for the parallel relation, which is also based on relative position measures and is adequate to represent the parallelism between a *globally* aligned group of objects and another object or group of objects. Illustrative examples on optical satellite images show the description power of these two relations and their combination for image interpretation.**

***Index Terms*—Alignment, fuzzy spatial relations, high-resolution remote sensing imaging, image interpretation, parallelism, spatial reasoning.**

I. Introduction

VERY high resolution remote sensing images (less than 1 m per pixel) allow us to discriminate different objects that compose a scene, such as buildings in an urban area or airplanes in an airport. However, recognizing individual objects is not enough to determine the semantics of a complex scene and to completely interpret it. Semantical scene understanding involves the assessment of the spatial arrangement of objects. Using spatial relations does not only help us discriminate the objects in the scene [1] but also allow us to distinguish between different interpretations of two scenes with similar objects but different spatial arrangements [2]. Some examples of the use of spatial relations can be found in the domain of medical imaging to recognize different brain structures [3], [4], in image interpretation to provide linguistic scene descriptions [5], in remote sensing imaging to classify or mine images [2], [6], in geographic information system applications to monitor land use [7], and land cover changes [8].

The spatial relations that are usually used to describe the spatial arrangement between image regions are topological relations as in [2] and [7]–[9], directional relations such as "to the right of" [2], [4], [5], [10], or distance relations [2], [4], [5], [11]. However, relations such as alignment have not been used so far in these works, although they can play an important role in image description. This is the case, for instance, in cartography, where it is necessary to find groups of aligned buildings for map generalization [12]. As another example, in object detection, complex semantic classes such as parking areas (car parking lots, harbors, truck parking lots, or airports) comprise aligned groups of vehicles. Thus, the identification of aligned groups of transport vehicles can be useful for detecting instantiations of these complex classes. Alignment is often linked to the parallel relation. For example, in object recognition, the aligned groups of airplanes in an airport are parallel to the terminal buildings, or the aligned groups of boats in a harbor are parallel to the deck. Another example is the determination of urban spatial patterns like groups of aligned houses parallel to other aligned groups of houses in residential areas.

We propose original definitions of parallelism and alignment as spatial relations between objects. Both are developed within the fuzzy set framework, in order to cope with the imprecisions that arise when these relations are evaluated between objects of different sizes for the case of alignment and different spatial extensions for the case of parallelism, as well as the imprecision obtained when measuring angles between points in a digital image. The proposed alignment relation is different from the definitions used in computer vision, which are based only on the barycenters of objects. Thus, it can be applied to objects of different sizes and whose barycenters are not necessarily aligned, which is often the case for several objects in remote sensing images. For the parallel relation, we propose a definition which considers the case where the relation takes place with a group of aligned objects or between objects of different lengths, which is useful for determining several man-made objects. Some of the ideas presented in this paper have been introduced in [13]–[15]. In this paper, we propose substantial

Manuscript received September 12, 2011; revised March 18, 2012 and July 9, 2012; accepted September 7, 2012. Date of publication December 10, 2012; date of current version May 16, 2013. This work was supported in part by the Centre National d'Etudes Spatiales–the German Aerospace Agency (DLR)–Télécom ParisTech Competence Center for Image Understanding and Information Extraction.

M. C. Vanegas was with Télécom ParisTech, 75634 Paris Cedex 13, France, and also with the Centre National d'Etudes Spatiales, 31400 Toulouse, France. She is now with Carestream Dental, 77435 Croissy-Beaubourg, France. (e-mail: carolina.vanegasorozco@carestream.com).

I. Bloch is with Télécom ParisTech, CNRS–LTCI UMR 5141, 75013 Paris, France (e-mail: isabelle.bloch@telecom-paristech.fr).

J. Inglada is with the Centre National d'Etudes Spatiales, 31400 France, and also with Centre d'Etudes Spatiales de la BIOsphère, 31401 Toulouse Cedex 9, France (e-mail: jordi.inglada@cesbio.cnes.fr).

Color versions of one or more of the figures in this paper are available online at http://ieeexplore.ieee.org.

Digital Object Identifier 10.1109/TGRS.2012.2225628

(a) (b) (c)

Fig. 1. Example of an aligned group of objects of different sizes and with nonaligned barycenters. (a) Original image. (b) Manually segmented objects. (c) Barycenters of objects in (b).

extensions of this preliminary work, with more developments, detailed algorithms, and examples.

This paper is organized as follows. In Section II, we review some of the models of alignment and parallelism between low-level features in computer vision and explain why they are not adequate for evaluating these relations as a high-level feature. In Section III, we introduce two new definitions for alignment, which are appropriate for the evaluation of objects found in remote sensing images. In addition, we propose an algorithm for extracting the groups of aligned objects. In Appendix, we explain the extension of the method to fuzzy objects. Section IV discusses the issues related to the definition of the parallel relation when dealing with objects or groups of aligned objects. An original definition of parallelism is then proposed, matching the requirements. Finally, in Section V, we apply the relations to objects in optical satellite images to illustrate their behavior and their usefulness in scene understanding.

II. Alignment and Parallelism in Computer Vision

Both parallelism and alignment between low-level features have been widely studied in computer vision. Some examples are parallelism between segments [16]–[22], alignment between groups of points [23], [24], and alignments between linear segments [16], [23] as colinearity in digital images. Most of these works are inscribed within the framework of perceptual organization. Their first objective is to find how to organize low-level features, such as edge segments, into groups, such as aligned segments or parallel segments. The groups are evaluated according to their perceptual significance based on the grouping laws of the gestalt theory [25], [26]. Their second objective is to differentiate the groupings that arise from the structure of a scene from those that arise due to accidents of view point or position [16].

Several methods to determine the *alignment* between points in a digital image have been proposed. Some of these methods rely on the Hough transform [23] or the Radon transform [27]. These methods can be directly used for objects by considering their barycenters, as in [23]. Another example, still relying on object barycenters, can be found in [28]. These representations are suitable mainly for small, convex, and regular objects, with similar sizes. However, when we reduce the object to a point, we lose all the shape information, which can lead to counter intuitive results, as shown in Fig. 1, where the objects should be considered as aligned according to their position, but their barycenters are not. Another example is the identification of aligned segments which have the same orientations as the alignment [16], [21], [23], [24], [29]. However, alignment extraction as a high-level feature has been less studied. One example is the work in [30], where an algorithm to detect groups of buildings with aligned barycenters in maps is presented. In this algorithm, the quality of the alignments is evaluated based on the criteria of proximity and similarity laws of the gestalt theory. The aforementioned methods for determining alignment focus on extracting groups of objects with aligned barycenters and on crisp objects. However, in remote sensing images, we can find groups of objects which are aligned, but their barycenters are not (see Fig. 1). Moreover, only considering the barycenters to determine their alignment is very sensitive to segmentation errors. Furthermore, when dealing with objects which have been extracted from images, it is important to consider alignment between fuzzy objects. Indeed, the object extraction processes can introduce imprecision, and therefore, we are not always dealing with crisp objects. Thus, it is necessary to propose a method which is robust to segmentation errors and capable of dealing with fuzzy objects, as well as alignments different from barycenters' alignment.

The relation of *parallelism* between two linear segments is usually modeled as a relation that should satisfy three constraints: 1) Both segments should have a small angular difference; 2) the perpendicular distance between the segments should be small; and 3) there should be a high overlap when one segment is projected into the other one and vice versa [17]. There exist different approaches to integrate these constraints into a model and measure the meaningfulness of the relation. Lowe [16] was one of the first to model parallelism to perform perceptual grouping: He assigned, to every pair of linear segments, a significance value, in order to establish if the parallelism was not originated by an accident on the viewpoint. This value is inversely proportional to the angular difference between the two segments and their perpendicular separation. In [17], the constraint about overlapping is introduced, and it is determined by the orthogonal projection of one segment over the other one and vice versa. The meaningful segments are then obtained by applying a threshold on the measured values of the constraints. Fuzzy approaches have been proposed in [19]–[21], [29], and [31], leading to a measure of the degree of parallelism between two linear segments, in which trapeze membership functions are used to evaluate to which degree the three constraints are satisfied. The three degrees are then combined in a conjunctive way. These works only consider parallelism between crisp segments. Nonetheless, as previously explained, it is important to consider parallelism between fuzzy linear objects. Moreover, parallelism and alignment have been addressed in an independent manner. However, when dealing with objects and observing these relations as spatial relations, it is interesting to combine them in order to determine when two groups of aligned objects are parallel or when a group of aligned objects is parallel to another object. These combinations give us more information about the scene and can be meaningful for obtaining a higher level description.

We propose two relations which can be used for image interpretation. Image interpretation is a high-level task, and to compute the relations, we assume that the objects have been previously segmented. Segmentation itself is a complex problem, and it is out of the scope of this work. However, we

consider that we cannot wait to have a perfect segmentation in order to proceed with the interpretation task. We can, for instance, start with an approximation of the objects by applying a segmentation method such as the ones in [32] and [33], or we can extract the objects by fusing different types of images as in [34] and [35] or simply use a dedicated method to extract desired objects as in [9] and [36]. Then, the results, even approximate, can be used for further image interpretation step. The proposed relations are capable of dealing with fuzzy objects. Moreover, we are aware that there is no algorithm which can provide a perfect segmentation; that is why we modeled our spatial relations within the fuzzy set framework which allows us to have a flexible definition able to extract the alignments even if objects have different sizes.

III. Alignment

Alignment can be defined as the spatial property possessed by a group of objects arranged in a straight line.[1] As it was highlighted by the gestalt theory, alignment should be seen as a whole [23]: If we observe each element of the group individually, then the alignment property is lost. Having to look at it as a whole makes alignment detection a difficult task, since, in order to detect an aligned group of objects, we have to identify its members, but to know if an object belongs to an aligned group, the alignment has to be already identified. First, let us describe the possible ways to model the alignment relation between objects by observing how alignment can be assessed in a set of points and then suggest how these approaches can be extended to deal with objects. Let $\mathcal{A} = \{a_1, \ldots, a_n\}$ be a set of points in $\mathbb{R}^2$. To determine whether the points of $\mathcal{A}$ are aligned, we can think of either of two equivalent strategies.

1) Perform a linear regression and search a line which is "near" all the points.
2) Find an angle $\theta \in [0, \pi[$ such that, for every pair of points a_i and $a_j (i \neq j)$, a_j is located in direction θ or $\theta + \pi$ from a_i with respect to the horizontal axis.

If we want to extend the first strategy to the case of objects, we can check whether the objects fall into a strip, and the thinner the strip, the better the alignment. However, the width of the strip will depend on the objects' sizes. Thus, the notion of falling into a thin strip is not appropriate for objects with different sizes. The difficulty of extending the second strategy relies on determining the angle between two objects. One alternative, which is the one proposed in this work, is to use measures of relative position used in spatial reasoning. Before entering into the details of the method, we introduce the notion of orientation histogram, inspired by the angle histogram of [37]. This notion is a fundamental concept for our method.

A. Angle and Orientation Histograms

Angle histograms were introduced in [37]. They can be interpreted as a function that captures the directional position between two objects. Suppose that we have two objects A and B defined by two regions in the image space $\mathfrak{I}$ that we also denote by A and B. The angle histogram from A to B is obtained by computing, for each pair of points $p \in A$ and $q \in B$, the angle between the vector $\vec{pq}$ joining them and a vector in the direction of the x-axis $\vec{u}_x$. Angles are organized in a histogram, normalized by the largest frequency

$$H^A(B)(\theta) = \frac{\sum \mathbf{1}_{\{(p,q)\in A\times B | \angle(\vec{pq},\vec{u}_x)=\theta\}}}{\max_{\phi\in[0,2\pi[} \sum \mathbf{1}_{\{(p,q)\in A\times B | \angle(\vec{pq},\vec{u}_x)=\phi\}}} \quad (1)$$

where $\mathbf{1}_X$ is the indicator function of the set X and $\angle(\vec{pq}, \vec{u}_x)$ denotes the angle between $\vec{pq}$ and $\vec{u}_x$. To determine if an object A is in a given direction with respect to an object B (for example, "right of"), we can compute the angle histogram $H^A(B)$ and compare it with a template of the relation "right of" by using, for instance, a conjunctive operator or the compatibility between the computed histogram and the template [37]. Angle histograms are also formalized for fuzzy objects. Given two fuzzy objects A and B defined through their membership functions $\mu_A : \mathfrak{I} \to [0, 1]$ and $\mu_B : \mathfrak{I} \to [0, 1]$ in the image space $\mathfrak{I}$, respectively, the angle histogram is defined as

$$H^A(B)(\theta) = \frac{\sum_{p,q\in\mathfrak{I} | \angle(\vec{pq},\vec{u}_x)=\theta} \mu_A(p) \wedge \mu_B(q)}{\max_{\phi\in[0,2\pi[} \sum_{p,q\in\mathfrak{I} | \angle(\vec{pq},\vec{u}_x)=\phi} \mu_A(p) \wedge \mu_B(q)} \quad (2)$$

where $\wedge$ denotes a triangular norm (fuzzy conjunction [38]), for example, the min function. When μ_A and μ_B are crisp, (2) and (1) are equivalent. Angle histograms take into account the shape of the regions, and thus, they provide an adequate way for evaluating the directional spatial relation between two objects [37]. In addition, they are invariant to simultaneous geometrical transformations of both objects.

We are interested in the orientation between two objects; thus, we introduce the orientation histogram, which is simply an angle histogram where the angles are computed modulo π

$$O(A,B)(\theta) = \frac{\sum_{p,q\in\mathfrak{I} | \mathrm{mod}(\angle(\vec{pq},\vec{u}_x),\pi)=\theta} \mu_A(p) \wedge \mu_B(q)}{\max_{\phi\in[0,\pi[} \sum_{p,q\in\mathfrak{I} | \mathrm{mod}(\angle(\vec{pq},\vec{u}_x),\pi)=\phi} \mu_A(p) \wedge \mu_B(p)}. \quad (3)$$

The orientation histogram is a fuzzy subset of $[0, \pi[$ that represents the orientation between two objects. It has the same properties as the angle histogram and, in addition, is symmetrical in A and B.

Similarity Degree for Orientation Histograms: To measure the degree to which two orientation histograms are similar, we can interpret the orientation histograms as fuzzy sets and use similarity measures based on aggregation [39], or we can consider the orientation histogram as a function and use a similarity degree based on a distance between functions. We decided to use a similarity degree based on intersection; nonetheless, other similarity measures are possible. More information on distances between histograms and similarity measures between fuzzy sets can be found in [39]–[41].

To determine the similarity degree between two histograms, we have to consider the imprecision that arises when computing angles between points in a discrete grid (which is the case

[1]Definition taken from ThinkMap Visual Thesaurus http://www.visualthesaurus.com/.

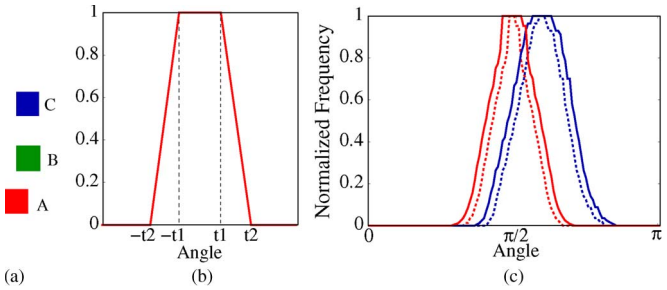

Fig. 2. (a) Objects. (b) Trapeze membership function. This function is parameterized by t_1 and t_2. (c) Orientation histograms of the objects in (a) in dotted lines and dilated orientation histograms in solid lines. The red orientation histograms represent the histograms from A to B, and the blue ones represent the histograms from B to C. For the dilation, we used a trapeze membership function with parameters $t_1 \approx \pi/36$ and $t_2 \approx 2\pi/45$ obtained by using $d_{\text{average}} = 10$ in (4) and (5).

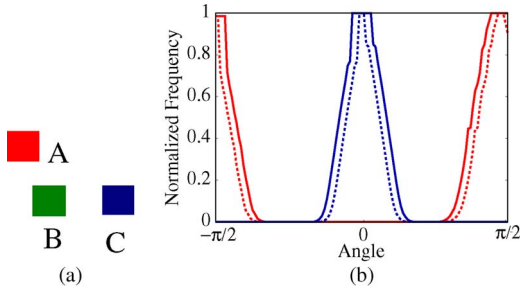

Fig. 3. Example of nonaligned objects. (a) Objects. (b) Orientation histograms of the objects in (a) and dilated orientation histograms. The red orientation histograms represent the histograms from A to B, and the blue ones represent the histograms from B to C. The dilated orientation histograms do not intersect.

for digital images). Moreover, when we refer to an orientation equal to an angle θ, it actually represents the quantity "approximately θ." To consider these sources of imprecision, we can perform a fuzzy morphological dilation [1] of $O(A, B)$ with a structuring element ν_0, where ν_0 is designed such that $\nu_0(\theta - \tilde{\theta})$ represents the degree to which $\tilde{\theta}$ and θ are "approximately" equal. Performing the dilation amounts to consider imprecision for all the angles in $O(A, B)$ (as in [42]), and the highest values of the histogram are propagated to the similar angle values according to ν_0. In our experiments, we modeled ν_0 as a symmetrical trapeze membership function [see Fig. 2(b)] with parameters t_1 and t_2, which are related to the approximation error induced when computing an angle between two points in an image. This error increases as the distance between the points gets smaller. Additionally, it also depends on the angle that is being computed. For a fixed distance, the largest error occurs around $\pi/4$, and the smallest one occurs around zero.[2] We define t_1 and t_2 as functions of the average distance d_{average} in pixels between the objects, in order to represent the minimum and maximum angle approximation errors which can occur, i.e.,

$$t_1 \approx \arctan\left(\frac{1}{d_{\text{average}} - 1}\right) \tag{4}$$

$$t_2 \approx \arctan\left(\frac{\left\lceil \frac{d_{\text{average}}}{\sqrt{2}} \right\rceil}{\left\lfloor \frac{d_{\text{average}}}{\sqrt{2}} \right\rfloor}\right) - \arctan\left(\frac{\left\lfloor \frac{d_{\text{average}}}{\sqrt{2}} \right\rfloor}{\left\lceil \frac{d_{\text{average}}}{\sqrt{2}} \right\rceil}\right). \tag{5}$$

Using a similarity measure based on aggregation [39], we define the degree of similarity between two orientation histograms $O(A, B)$ and $O(C, D)$ as the maximum height of the fuzzy intersection of their dilations

$$\text{sim}((O(A,B), O(C,D)) = \max_{\theta \in [0,\pi[} \left[D_{\nu_0}\left(O(A,B)\right)(\theta) \wedge D_{\nu_0}\left(O(C,D)\right)(\theta) \right] \tag{6}$$

[2]This can be verified by plotting the approximation error in function of the angle, using a fixed distance between the points. For a fixed distance d between two points and an angle θ, the maximum approximation error is equal to $\arctan(\lceil d_y \rceil / \lfloor d_x \rfloor) - \arctan(\lfloor d_y \rfloor / \lceil d_x \rceil)$, where d_x and d_y are the horizontal and vertical distances, respectively, obtained as $d_x = d\cos(\theta)$ and $d_y = d\sin(\theta)$. It is enough to plot the function in the interval $[0, \pi/4]$, since the other approximation errors are deduced by symmetry.

where $D_{\nu_0}(O(X, Y))$ is the fuzzy morphological dilation of $O(X, Y)$ by a structuring element ν_0, given by $D_{\nu_0}(\mu)(\theta) = \sup_{\tilde{\theta} \in [0,\pi[} \min(\mu(\tilde{\theta}), \nu_x(\theta - \tilde{\theta}))$ [1]. Fig. 2(c) shows, in dotted lines, the orientation histograms for the objects of Fig. 2(a) and, in solid lines, the dilated orientation histograms. The similarity value between the histograms using (6) is 0.93, which is consistent with the perceived orientation of the objects. If we had not considered the different sources of imprecision, then the similarity degree would have been the maximum of the intersection of the two orientation histograms, i.e., 0.67, which is not in agreement with the situation.

When the orientation histograms are not similar (see Fig. 3), we obtain a zero similarity value, as desired. This similarity measure can be extended to compare several orientation histograms. Let $\{O(A_i, A_j)\}_{i=0, j \neq i}^{N}$ be a set of orientation histograms; we define the similarity degree between them as

$$\text{sim}\left(O(A_0, A_1), \ldots, O(A_i, A_j), \ldots O(A_N, A_{N-1})\right) = \max_{\theta \in [0,\pi[} \bigwedge_{i=0, j \neq i}^{N} D_{\nu_0}\left(O(A_i, A_j)\right)(\theta). \tag{7}$$

B. Definition of Aligned Groups of Objects

Before proposing a definition of alignment, we define preliminary concepts on neighborhoods. Let $\mathcal{S}$ be a group of objects. For $A, B \in \mathcal{S}$, we define the $\text{Neigh}(A, B)$ relation as being satisfied if and only if $B \cap A = \emptyset$ and $B \cap N(A) \neq \emptyset$, where $N(A)$ is defined as a neighborhood of A. Some examples of neighborhoods for an object A are $N(A) = V_d(A)$, where $V_d(A)$ is the Voronoï neighborhood constrained by a distance d, or $N(A) = N_d(A)$, where $N_d(A) = \{x \in \Im | \text{dist}(x, A) \leq d\}$, i.e., all the points which are at a distance less than d from A. Other possible choices are discussed in Appendix.

Definition 3.1: A group $\mathcal{S}$ is called connected by the *Neigh* relation if, for every $A, B \in \mathcal{S}$, there exist $C_0, \ldots, C_M$ objects in $\mathcal{S}$, such that $C_0 = A$, $C_M = B$, and, for every $m = 0, \ldots, M - 1$, the relation $\text{Neigh}(C_m, C_{m+1})$ is satisfied. According to the semantic meaning of the alignment relation, the group $\mathcal{S}$ is aligned if the following conditions are satisfied.

1) $\mathcal{S}$ is connected by the *Neigh* relation.
2) $|\mathcal{S}| \geq 3$.

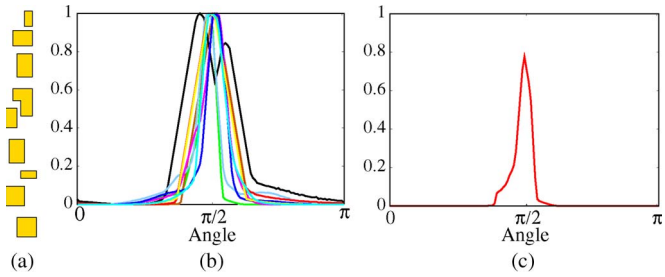

Fig. 4. (a) Group of objects for which the orientation between the fifth and sixth objects (counting from the bottom) is different from the orientation between the other pairs of objects of the group. (b) The dilated orientation histograms $D_{\nu_0}(O(A_i, \mathcal{S} \setminus \{A_i\}))$ for objects in (a), using the same structuring element to perform the dilation of each histogram. (c) Aggregation of the histograms in (b) using the t-norm of Lukasiewicz ($a \wedge b = \max(0, a + b - 1)$).

3) There exists $\theta \in [0, \pi[$ such that, for every $A \in \mathcal{S}$, A is able to see the rest of the group in direction θ or $\theta + \pi$ with respect to the horizontal axis.

The first condition ensures that the consecutive members of the group are neighbors and, thus, that the group is not "divided." The second condition states that an aligned group should have at least three elements. To verify the third condition, we measure that all the orientation histograms $O(A_i, \mathcal{S} \setminus \{A_i\})$ are similar for all $A_i \in \mathcal{S}$. For any $A_i \in \mathcal{S}$, the histogram $O(A_i, \mathcal{S} \setminus \{A_i\})$ represents the orientation between A_i and the rest of the group. This measure is robust with respect to small deviations in the group. For instance, if two pairs of objects of the group have dissimilar orientations but there is still a general tendency of alignment within the group, then the orientation dissimilarity between these pairs will not affect the whole conjunction, because the comparison is done between the orientations of the whole group with respect to its members. The group in Fig. 4(a) has a pair of objects with an orientation different from the orientations between the other pairs. However, there is a tendency in the orientation of the whole group. This tendency is reflected in the dilated histograms $D_{\nu_0}(O(A_i, \mathcal{S} \setminus \{A_i\}))$ of Fig. 4(b) and in their aggregation in Fig. 4(c), which gives a similarity measure of 0.81. Thus, it is possible to define the degree of alignment as follows.

Definition 3.2: Let $\mathcal{S} = \{A_0, \ldots, A_N\}$, with $N \geq 3$, be a group of objects in $\mathfrak{I}$, connected by the *Neigh* relation. Then, the degree of alignment of $\mathcal{S}$ is given by

$$\mu_{\mathrm{ALIG}}(\mathcal{S}) = \mathrm{sim}(O(A_0, \mathcal{S} \setminus \{A_0\}), \ldots, O(A_N, \mathcal{S} \setminus \{A_N\})).$$

As shown in Fig. 4, this definition is appropriate for measuring the degree of alignment of groups. However, if we want to find the aligned groups of objects within a set of objects, then this measure is not enough, since it would be necessary to measure the degree of alignment for every group connected by the *Neigh* relation with more than three members than can be formed from the set. Therefore, we propose to introduce a local measure which helps determine the candidates for being an aligned group of objects. This measure is called *local* alignment, and the one in Definition 3.2 is called *global* alignment.

Definition 3.3: Let $\mathcal{S} = \{A_0, \ldots, A_N\}$, with $N \geq 3$, be a group of objects in $\mathfrak{I}$, connected by the *Neigh* relation. The degree of *local* alignment of $\mathcal{S}$ is given by

$$\mu_{\mathrm{LA}}(\mathcal{S}) = \min_{\substack{X,Y,Z: \\ \mathrm{Neigh}(X,Y) \wedge \mathrm{Neigh}(Y,Z)}} \mathrm{sim}(O(X,Y), O(Y,Z)).$$

The degree μ_{LA} measures that, for every pair of elements $B, C \in \mathcal{S}$ belonging to $N(A)$, the orientations $O(A, B)$ and $O(A, C)$ are similar. We will say that a group of objects $\mathcal{S}$ is *locally* aligned to a degree β if $\mu_{\mathrm{LA}}(\mathcal{S}) \geq \beta$.

C. Identification of Locally Aligned Groups

Summarizing Definition 3.3, we can say that a group $\mathcal{S}$ with $|\mathcal{S}| \geq 3$ is *locally* aligned to a degree β if it satisfies

$$\begin{aligned} R1 &: \forall X, Y, Z\, (\mathrm{Neigh}(X,Y) \wedge \mathrm{Neigh}(Y,Z)) \\ &\quad \Rightarrow (\mathrm{sim}(O(X,Y), O(Y,Z)) \geq \beta) \\ R2 &: \forall A, B, \exists X_0, \ldots, X_m \text{ such that} \\ &\quad X_0 = A, X_m = B \text{ and } \left(\bigwedge_{i=0}^{m-1} \mathrm{Neigh}(X_i, X_{i+1}) \right). \end{aligned}$$

Thus, the notion of *local* alignment depends on the *Neigh* relation. To determine the objects which are connected through the *Neigh* relation, we propose to construct a neighborhood graph $G_N = (\mathcal{V}, E)$ where the vertices represent the objects, and there is an edge between two vertices if the corresponding objects are neighbors. Notice that only the connected subsets of three vertices X, Y, and Z in G_N which share a common vertex, for example, Y, satisfy the condition $\mathrm{Neigh}(X,Y) \wedge \mathrm{Neigh}(Y,Z)$. We call these connected subsets *triplets*. According to $R1$, the *triplets* $\{X, Y, Z\}$ which satisfy $\mathrm{sim}(O(X,Y), O(Y,Z)) \geq \beta$ are aligned and can belong to a *locally* aligned group to a degree β. *Triplets* can be easily identified as the edges of the dual graph $\tilde{G}_N = \{\tilde{\mathcal{V}}, \tilde{E}\}$ of G_N, when it is constructed in the following manner. Each vertex $\tilde{V}_i \in \tilde{\mathcal{V}}$ represents an edge in the graph G_N. There is an edge between the vertices $\tilde{V}_i$ and $\tilde{V}_j$ of $\tilde{G}_N$ if the corresponding edges of the graph G_N have a common vertex. If, additionally, we attribute to each edge (i, j) the similarity degree between the orientation histograms of $\tilde{V}_i$ and $\tilde{V}_j$ that we denote by $\tilde{s}_{ij}$, then it is possible to verify if relation $R1$ holds for its corresponding *triplet*. Fig. 5 shows an example of a neighborhood graph and its dual graph. Notice that the edges of $\tilde{G}_N$ with a high value represent the *triplets* of objects with similar orientation histograms. For instance, in the dual graph, the edge between the nodes (1–2) and (2–3) has a similarity value of one, and this edge corresponds to the objects labeled 1, 2, and 3 of Fig. 5(a). In a similar way, edges with a low value represent objects which are not aligned; for example, in the dual graph, the edge between the nodes (1–2) and (6–2) has a similarity value of 0.11 and corresponds to the objects labeled 1, 2, and 6, which do not form a *locally* aligned *triplet*.

Returning to the conditions of *local* alignment $R1$ and $R2$, the first one states that *triplets* should be *locally* aligned, and the second one states that the group should be formed by connected objects according to the *Neigh* relation. A group $\mathcal{S}$ fulfills these

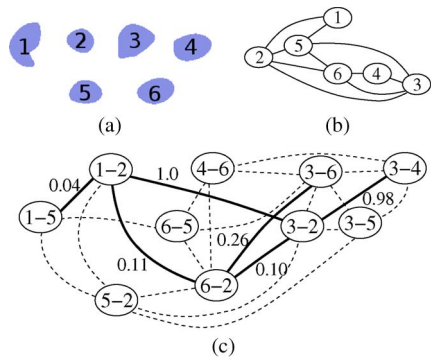

Fig. 5. (a) Objects. (b) Neighborhood graph of the objects in (a) using a Voronoï neighborhood. (c) Dual graph of (b). For clarity purpose, the edges with an edge value equal to zero are drawn in dotted lines, and those with an edge value greater than zero are in solid lines. We only indicate the edge value when it is greater than zero.

conditions if and only if the subset $\tilde{\mathcal{S}} \subseteq \tilde{\mathcal{V}}$ which represents the dual of $\mathcal{S}$ satisfies

$$\tilde{R}1 : \forall \tilde{V}_i, \tilde{V}_j \ \text{Connected}(\tilde{V}_i, \tilde{V}_j) \Rightarrow (\tilde{s}_{ij} \geq \beta)$$

$$\tilde{R}2 : \forall \tilde{V}_i, \tilde{V}_j \exists \tilde{U}_0, \ldots, \tilde{U}_K \text{ for } K \geq 1 \text{ such that}$$

$$\tilde{U}_0 = \tilde{V}_i, \tilde{U}_N = \tilde{V}_j \text{ and } \bigwedge_{k=0}^{K-1} \text{Connected}(\tilde{U}_0, \tilde{U}_k)$$

where $\text{Connected}(\tilde{U}, \tilde{V})$ is true if there exists an edge between $\tilde{U}$ and $\tilde{V}$. Condition $\tilde{R}2$ expresses that $\tilde{\mathcal{S}}$ should be connected, since if $\tilde{\mathcal{S}}$ is not connected, then $\mathcal{S}$ is not connected. Consequently, a *locally* aligned group is a subset $\mathcal{S} \subseteq \mathcal{V}$ for which its dual set $\tilde{\mathcal{S}} \subseteq \tilde{\mathcal{V}}$ is connected in $\tilde{G}$ and the value of all the edges joining the vertices within $\tilde{\mathcal{S}}$ is greater than or equal to β.

The algorithm shown in Fig. 7 can be used to extract the $\tilde{\mathcal{S}}_i \subset \tilde{\mathcal{V}}$ corresponding to the dual sets of the *locally* aligned sets $\mathcal{S}_i \subset \mathcal{V}$. First, the connected components of a graph $\tilde{G}_{\text{TH}}$ are computed and stored in $\mathfrak{C}$. $\tilde{G}_{\text{TH}}$ is a nonattributed graph containing all the vertices of $\tilde{G}$, and there is an edge between two vertices if the edge in $\tilde{G}$ has a value greater than or equal to β. Then, for each component $\mathcal{C}_k$, we compute the minimum value of its edges in $\tilde{G}$ that we call consistency degree of C_k and denote by $\text{cons}(\mathcal{C}_k) = \min\{\tilde{s}_{ij} | \tilde{V}_i, \tilde{V}_j \in \mathcal{C}_k\}$. If $\text{cons}(\mathcal{C}_k) < \beta$, then $\mathcal{C}_k$ does not satisfy $\tilde{R}1$; thus, vertices are removed until $\text{cons}(\mathcal{C}_k) \geq \beta$. If, in the process of vertex removal, $\mathcal{C}_k$ becomes disconnected, then each of the connected components of $\mathcal{C}_k$ is processed separately. The vertices which are removed are the ones having more conflict with their neighbors in $\mathcal{C}_k$. We say that two connected vertices $\tilde{V}_i$ and $\tilde{V}_j$ are in conflict if $\tilde{s}_{ij}$ is close to zero, i.e., if the corresponding orientation histograms of both vertices are not similar. The conflict of a vertex $\tilde{V}_t$ with its neighbors in $\mathcal{C}_k$ is measured by using what we call the degree of the vertex in $\mathcal{C}_k$

$$\deg(\tilde{V}_t) = \frac{\sum_{\tilde{V}_j \in \mathcal{C}_k} \tilde{s}_{tj}}{\left| \left\{ (t,j) | \tilde{V}_j \in \mathcal{C}_k \right\} \right|}. \tag{8}$$

This degree represents the average edge value over all the edges connected to $\tilde{V}_t$. It is clear that if $\tilde{V}_t$ is in conflict with several of its connected vertices in $\mathcal{C}_k$, then $\deg(\tilde{V}_t)$ will be close to zero, and it will be close to one if there is no conflict. Then, the conflict of a vertex will be given by $1 - \deg(\tilde{V}_t)$. Fig. 6

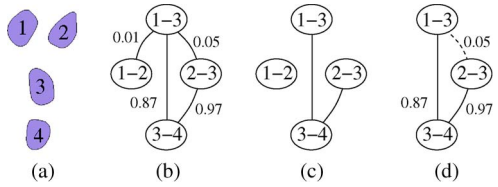

Fig. 6. Conflict illustration: (a) Group of objects which are in conflict. (b) Dual graph of objects in (a). (c) $\tilde{G}_{\text{TH}}$ for $\beta = 0.8$. $\tilde{G}_{\text{TH}}$ contains one connected component composed of the vertices (1–3), (2–3), and (3–4) with a consistency degree of 0.05, which is inferior to β. (d) Vertices of the connected component of $\tilde{G}_{\text{TH}}$ seen by $\tilde{G}$. This component has a consistency degree of 0.05.

shows an example where there is a conflict between the vertices of a connected component for $\beta = 0.8$. $\tilde{G}_{\text{TH}}$ contains one connected component. Fig. 6(c) shows the thresholded graph, which has a consistency degree of 0.05, which is inferior to β. The conflict of the nodes (1–3), (2–3), and (3–4) are 0.54, 0.49, and 0.08, respectively. Therefore, the nodes (1–3) and (2–3) have a conflict with their neighbors in this component. Removing the vertex (1–3), which is the one with the higher conflict, leads to a consistency degree of $\text{cons}(C_0) = 0.89$, which is now larger than $\beta = 0.8$.

In Appendix, we explain how the method for detecting *locally* aligned groups of objects is extended to the cases where we use a fuzzy neighborhood.

D. Candidates for Globally Aligned Groups

To obtain the *globally* aligned groups to a degree β, we first extract the *locally* aligned groups to a degree β. For every *locally* aligned group $\mathcal{S}$, we evaluate the degree of *global* alignment using Definition 3.2. If $\mu_{\text{ALIG}}(\mathcal{S}) < \beta$, then we divide the group by eliminating the vertices in $\tilde{\mathcal{S}}$ with the minimum vertex degree (8) in $\tilde{\mathcal{S}}$, until $\mu_{\text{ALIG}}(\mathcal{S}) \geq \beta$. If the degree of all vertices in $\tilde{S}$ is equal to one and $\mu_{\text{ALIG}}(\mathcal{S}) < \beta$, it means that a lot of imprecision was introduced for the similarity computation, and the measurement of similarity is very permissive; thus, the whole process should be repeated using a ν_0 with a tighter support in (7). Note that this step was not necessary in our experiments.

E. Interpreting the Degree of Alignment

The degree of alignment of a group determines the flexibility of the notion of alignment in the group. To better understand the significance of this degree, we extracted several groups of *globally* aligned buildings from the buildings in Fig. 8(b) using different values of β. The resulting groups, as well as their degrees, are given in Fig. 8(c)–(m). From the results, we can see that the groups with a lower degree, for instance, the group of Fig. 8(d), are in fact not aligned. The groups of Fig. 8(e)–(m) have very high degrees of alignment and are well aligned. The group in Fig. 8(c) has a degree of alignment of 0.75, and we can notice that the objects in the group do not follow a perfect alignment; meanwhile, we can see that there is a strong tendency into a direction and this is reflected by the obtained degree. Therefore, according to the situation that we want to represent, we can choose an adequate value of β. For $\beta \approx 0.6$, we obtain flexible alignments as the ones in Fig. 8(c)

Input: Dual graph $\tilde{G}$, β
Output: $\mathfrak{L}$
  Create $\tilde{G}_{TH} = (\tilde{\mathcal{V}}, \tilde{E}_{TH})$, where $\tilde{E}_{TH} = \{(i,j) \in \tilde{E} \mid \tilde{e}_{ij} \geq \beta\}$
  Find $\mathfrak{C}$ the set of connected components of $\tilde{G}_{TH}$
  for all $\mathcal{C}_k \in \mathfrak{C}$ **do**
    $cons \leftarrow \min\{\tilde{s}_{ij} \mid \tilde{V}_i, \tilde{V}_j \in \mathcal{C}_k\}$
    while $cons < \beta$ and $|\mathcal{C}_k| \geq 2$ **do**
      for all $\tilde{V}_t \in \mathcal{C}_k$ **do**
        $deg_t \leftarrow \frac{\sum_{\tilde{V}_j \in \mathcal{C}_k} \tilde{s}_{tj}}{|\{(t,j) | \tilde{V}_j \in \mathcal{C}_k\}|}$
      end for
      Delete from $\mathcal{C}_k$ the $\tilde{V}_j$ for which $\tilde{V}_j = \min_{\tilde{V}_i \in \mathcal{C}_k} deg_i$
      if C_k is disconnected in $\tilde{G}_{TH}$ **then**
        Let $\mathfrak{D} = \{\mathcal{D}_0, \ldots, \mathcal{D}_L\}$ the connected components of $\mathcal{C}_k$
        $\mathcal{C}_k \leftarrow \mathcal{D}_0$
        for $l = 1$ to L **do**
          $\mathfrak{C} \leftarrow \{\mathcal{D}_l\} \cup \mathfrak{C}$
        end for
        $cons \leftarrow \min\{\tilde{s}_{ij} \mid \tilde{V}_i, \tilde{V}_j \in \mathcal{C}_k\}$
      end if
    end while
    if $cons \geq \beta$ **then**
      $\mathfrak{L} \leftarrow \{\mathcal{C}_k\} \cup \mathfrak{L}$
    end if
  end for

Fig. 7. Algorithm for finding locally aligned groups $\mathfrak{L}$ from $\tilde{G}$.

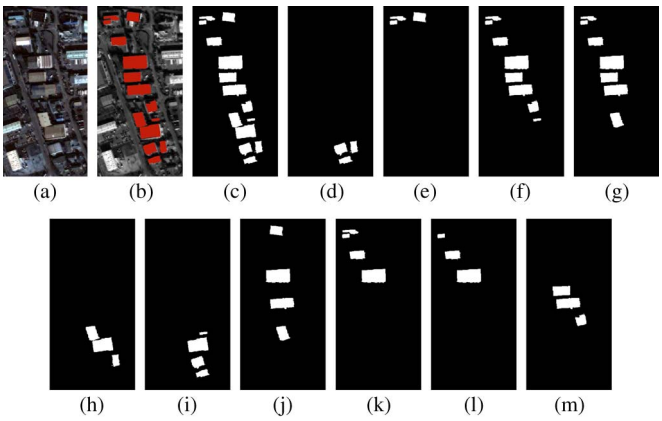

Fig. 8. (a) Original image. (b) Buildings for which we extracted the groups shown in (c)–(m). The degrees of *global* alignment of each group are 0.75 (c), 0.3 (d), 0.97 (e), 0.98 (f), 0.96 (g), 0.98 (h), 0.93 (i), 1.0 (j), 0.97 (k), 1.0 (l), and 0.98 (m).

and more strict alignments as in Fig. 8(e)–(m). For $\beta \approx 0.8$, we obtain strict alignments only.

Let $\mathcal{S}_1$ and $\mathcal{S}_2$ be two groups of *globally* aligned objects with degrees of alignment β_1 and β_2, respectively, such that $\mathcal{S}_1 \subseteq \mathcal{S}_2$ and $\beta_1 \geq \beta_2$. If we search for the *globally* aligned groups using $\beta = \beta_1$, then only group $\mathcal{S}_1$ will be obtained, and similarly, if we used $\beta = \beta_2$, then only $\mathcal{S}_2$ will be obtained. This is because algorithm in Fig. 7 searches for the largest *locally* aligned group which has a degree larger than β. Therefore, if we want to have groups with a degree greater than β_2 and its subgroups, then algorithm in Fig. 7 should be applied with increasing values of β starting from β_2 until 1.0. One example of this situation is the groups in Fig. 8(c) and (f).

F. Adding More Elements to the Group

Once the *globally* aligned groups of objects are identified, it is possible to add new objects to the group or fuse two *globally* aligned groups to obtain a larger one. We add an object B to a group $\mathcal{S}$, if B satisfies the *Neigh* relation with a member of $\mathcal{S}$ and if it is located in the direction of the alignment of $\mathcal{S}$. Similarly, we fuse two groups $\mathcal{S}$ and $\mathcal{T}$, if both have similar orientations [according to (7)], if there is a member of $\mathcal{S}$ which satisfies the *Neigh* relation with a member of $\mathcal{T}$, and if all the members of $\mathcal{S}$ are located in the direction of the alignment of $\mathcal{T}$. The direction of alignment of a group is defined as the angle which maximizes the conjunction of the dilated orientation histograms $D_{\nu_0} O(A_i, \mathcal{S} \setminus \{A_i\})$. To determine whether an object is located in the direction of the alignment of a group, we use a directional dilation [1]. The directional dilation of a fuzzy set μ in a direction $\vec{u}_\phi$ is defined as [1]

$$D_{\nu_\phi}(\mu)(x) = \sup_y \min\left[\mu(y), \nu_\phi(x-y)\right] \tag{9}$$

where ν_ϕ is a fuzzy directional structuring element chosen so as to have high membership values in the direction $\vec{u}_\phi$ and its value at a point $x = (r, \alpha)$ (in polar coordinates) is a decreasing function of $|\phi - \alpha|$ modulo 2π. Therefore, to determine whether an object B is located in the direction of alignment θ of a group $\mathcal{S}$, we perform two directional dilations of $\mathcal{S}$ in the directions $\vec{u}_\theta$ and $\vec{u}_{\theta+\pi}$ and evaluate the degree to which B is included in the region obtained from the union of the two dilations using a degree of inclusion [1]. The degree of inclusion of a fuzzy set μ in a fuzzy set ν is defined as

$$\mu_{\text{inclusion}}(\mu, \nu) = \inf_{x \in \mathfrak{I}} \left((1 - \mu(x)) \vee \nu(x)\right) \tag{10}$$

where $\vee$ denotes a triangular conorm (fuzzy disjunction [38]), for example, $\vee = \max$.

Fig. 9 shows a *locally* aligned group which has been extended to add more elements.

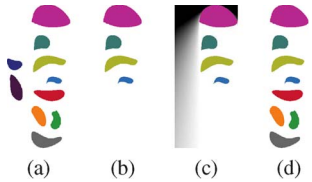

Fig. 9. (a) Objects. (b) An aligned group having a degree of *local* alignment of 0.9 and *global* alignment of 0.85. (c) Directional dilations of the group in (b) in alignment direction (white represents a high value of visibility). (d) Group obtained after adding new elements, with a degree of *global* alignment of 0.8.

G. Stability With Respect to Segmentation Errors

One interesting feature of our approach is that it is robust to the quality of the segmentation of the objects. This property is particularly important in real applications where it is difficult to guarantee that all objects have been adequately segmented. Fig. 10(b) shows a correct segmentation of the houses of Fig. 10(a). In Fig. 10(d), we manually introduced two segmentation errors: absence of objects and the merging of an undesired region to one of the objects. For both cases, we extracted the *globally* aligned groups using the same extraction parameters and a Voronoï neighborhood constrained by a distance of 50 pixels. Some of the obtained groups are shown in Fig. 10(c) for Fig. 10(b) and in Fig. 10(e) for Fig. 10(d).

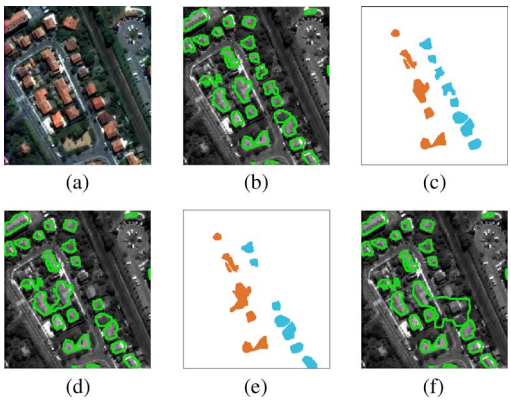

Fig. 10. (a) Original image. (b) Green lines show the boundaries of the segmented houses. (c) Some of the extracted *globally* aligned groups from objects of (b). More groups are extracted by the algorithm, but for the sake of clarity, only a few groups are shown. For both groups, we have that $\mu_{\mathrm{ALIG}} = 1.0$. (d) Segmented houses with errors of missing objects and some merged regions. (e) Some of the extracted *globally* aligned groups from objects of (d). The left group has a degree of alignment $\mu_{\mathrm{ALIG}} = 0.94$, and the right one has a degree $\mu_{\mathrm{ALIG}} = 1.0$. (f) Example of segmentation error that does not allow the recovery of the *globally* aligned groups.

We can see that the two groups are retrieved in both cases, even in the presence of the introduced segmentation errors. The degrees of *global* alignment remained almost the same, since the missing objects and the modification of the object are local changes which do not affect the *global* orientation of the groups. However, we should notice that if we had used a neighborhood constrained to a smaller distance, then the algorithm would not have retrieved the group with the missing objects, since there would have been a disconnection between the upper and lower parts of the group. Moreover, if one of the objects is severely modified as in Fig. 10(f), then it is not possible to retrieve the same aligned groups as before. These two types of behaviors were actually expected.

H. Complexity Analysis

In this section, we deal with the cost of the basic operations of the algorithm for extracting *locally* aligned groups and *globally* aligned groups. Suppose that we have N objects, each with at most n_o points, and that the image has at most N_I points. The complexity of extracting the *locally* aligned groups is $O(N^2)$ since most of the steps of the algorithm deal with operations over the graph or its dual. However, it should be noticed that the construction of the orientation histograms has a complexity of $O(N^2 n_o^2)$, since there is a maximum of $N(N-1)$ edges in the graph and, for each edge, an orientation histogram is constructed with a complexity of $O(n_o^2)$. Given a *locally* aligned group with N_A elements each having at most n_o points, then the complexity of finding a *globally* aligned group is $O(N_A^2 n_o^2 + N_I)$. The complexity of evaluating μ_{ALIG} and dividing the group in the case where it is not aligned is $O(N_A^2 n_o^2)$. Additionally, the complexity of adding more objects to the group is $O((N - N_A)n_o^2 + N_I)$, where the complexity of the directional dilation is $O(N_I)$ [43][3] and the complexity of evaluating the degree of inclusion of each object not belonging to the group into the directional dilations of the group is $O((N - N_A)n_o^2)$. Overall, the final global complexity is $O(N^2 n_o^2)$ (quadratic in N and n_o).

[3]See [43] for the implementation of the directional morphological dilation using a propagation method.

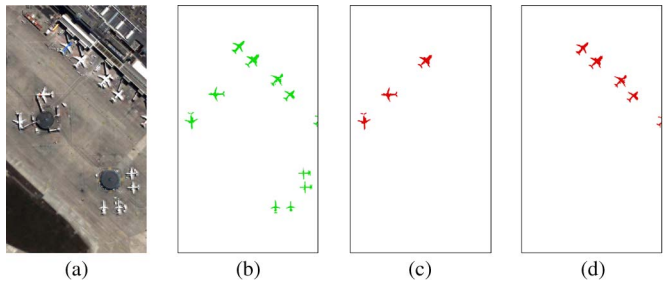

Fig. 11. (a) Airport image. (b) (Green) Manually segmented airplanes. (c) Extracted *globally* aligned group in red with degree 0.97. (d) Extracted *globally* aligned group in red with degree 0.99.

Finally, let us mention that some steps can be computed in a fast way, using updating or approximation processes. This is typically the case for the computation of histograms. For instance, an orientation histogram can be easily updated when a new object is added to or removed from a group, without any recomputation for the other objects. This update process is not computationally expensive, if we store the value used to normalize the orientation histogram, i.e., the denominator of (3). Let $\mathcal{S} = \{A_0, \ldots, A_N\}$ be a *globally* aligned group and suppose that we want to know if an object B can be added to the group; then, we have to compute the following orientation histograms: $O(B, \mathcal{S})$ and $O(A_i, B \cup \mathcal{S} \setminus \{A_i\})$ for every $A_i \in \mathcal{S}$. However, if we compute $O(B, A_i)$ for every $A_i \in \mathcal{S}$, the histograms can be easily updated as

$$O\left(A_i, B \cup \mathcal{S} \setminus \{A_i\}\right)(\theta) = \frac{g(\theta)}{h}$$

where $g(\theta) = O(A_i, \mathcal{S} \setminus A_i)(\theta) \cdot \mathrm{den}(O(A_i, \mathcal{S} \setminus A_i)) + O(B, A_i)(\theta) \cdot \mathrm{den}(O(B, A_i))$, $h = \max_{\phi \in [0,\pi]}[O(A_i, \mathcal{S} \setminus A_i)(\phi) \cdot \mathrm{den}(O(A_i, \mathcal{S} \setminus A_i))O(B, A_i)(\phi) \cdot \mathrm{den}(O(B, A_i))]$, and $\mathrm{den}(O(A, B))$ is the value used for the normalization of the orientation histogram $O(A, B)$.

Moreover, the computation can be faster using approximations of the objects, for instance, using subsampling, which may lead to sufficient precision in practice.

I. Discussion

In this first part, we have introduced the definitions of *global* alignment and underlined the need of introducing the definition of *local* alignment. We proposed an algorithm for extracting the *locally* aligned groups from an image of segmented objects. We have illustrated that these definitions are adequate for determining the alignments of objects of different sizes and whose barycenters are not necessarily aligned. However, the obtained groups only satisfy the conditions of alignment and thus may not be meaningful enough for the description of the scene.

For example, Fig. 11 shows two *globally* aligned groups of airplanes extracted using the proposed algorithm; the group of Fig. 11(c) is *globally* aligned but does not give any information about the arrangement of the airplanes, while the group of

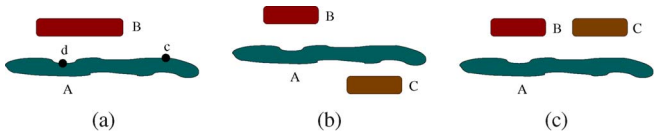

Fig. 12. Examples where parallelism should preferably be considered as a matter of degree and should not be necessarily symmetrical and transitive.

Fig. 11(d) gives us more information about the arrangement of the airplanes. Therefore, it is necessary to use additional information to put the aligned groups into context, for example, finding whether the alignments are parallel between them or parallel to another object. In the case of Fig. 11, it is interesting to find the groups which are parallel to the buildings. This point will be further discussed in the next section.

We proposed an algorithm which is very flexible, in the sense that it allows the incorporation of more information according to the type of alignment. For example, if we are searching for an alignment where the objects of the alignment have the same orientation as the alignment, this could be incorporated in the weights $\tilde{s}_{ij}$ assigned to the edges of the dual graph. The new weight $\tilde{s}_{ij}$ of the edge between the vertices $\tilde{V}_i$ and $\tilde{V}_j$, representing a *triplet* $\{X, Y, Z\}$, is given by the conjunction of combining the condition that $O(X, Y)$ and $O(Y, Z)$ are similar and the condition that every member of the *triplet* has a similar orientation to the orientation histograms between itself and its neighbors within the triplet. For instance, assuming that Y is connected to X and Z, this condition is expressed as follows: $\mathrm{sim}(O(X, Y), \delta_{\theta_Y}) \wedge \mathrm{sim}(O(Z, Y), \delta_{\theta_Y})$, where θ_Y is Y's orientation and δ_{θ_Y} is the Dirac function at this angle. For X and Z, the condition is verified only with the histograms that involve them, i.e., $O(X, Y)$ and $O(Z, Y)$, respectively. Finally, when combining all the conditions, the weight $\tilde{s}_{ij}$ becomes

$$\begin{aligned}\tilde{s}_{ij} = &\,\mathrm{sim}\left(O(X,Y), O(Y,Z)\right) \\ &\wedge[\min\left[\mathrm{sim}\left(O(X,Y), \delta_{\theta_Y}\right) \wedge \mathrm{sim}\left(O(Z,Y), \delta_{\theta_Y}\right)\right. \\ &\left.\mathrm{sim}\left(O(X,Y), \delta_{\theta_X}\right), \mathrm{sim}\left(O(Z,Y), \delta_{\theta_Z}\right)\right]].\end{aligned}$$

To ensure that the second condition is satisfied by all the members of the *triplet*, we used a min operator to aggregate all the conditions. This example illustrates how we can easily introduce additional information into the proposed model in order to better satisfy the semantics of the desired relation.

IV. Parallelism

For linear objects to be parallel, we expect a constant distance between them or that they have the same normal vectors and the same orientation. Although classical parallelism in Euclidean geometry is a symmetric and transitive relation, these properties are subject to discussion when dealing with linear objects of finite length. When objects have different extensions as in Fig. 12(a), where B can be a house and A can be a road, the symmetry becomes questionable. The statement "B is parallel to A" can be considered as true, since, from every point on the boundary of B that faces A, it is possible to see (in the normal direction to A's principal axis) a point of A, and the orientations of A and B are similar. On the other hand, the way we perceive "B parallel to A" changes depending on our position: From point d, it is possible to see a point of B in the normal direction of B, while this is not possible from point c. With similar arguments, we can show that the transitivity is lost. For example, in Fig. 12(b) and (c), the statements "B is parallel to A" and "A is parallel to C" hold, but "B is not parallel to C." Moreover, these examples illustrate the ambiguity of the relation and the interest of considering it as a degree of satisfaction rather than a crisp relation.

As discussed in Section II, the parallel relation can also be considered between a group of objects $\mathcal{A} = \{A_i\}$ and an object B, typically when the objects in the group are *globally* aligned and B is elongated, for example, a group of boats and a deck in a harbor. When evaluating the relation "$\mathcal{A}$ is parallel to B," we are evaluating whether the whole set $\mathcal{A}$ and the boundary of B that faces $\mathcal{A}$ have a similar orientation and whether there is a large proportion of the group that sees B in the normal direction to the group. Similar considerations can be derived when considering the relation "B is parallel to $\mathcal{A}$" or the relation between two groups of objects. All these considerations form the basis for the formal models provided in this section.

For "A to be parallel to B," it is only necessary that A is a linear object, while B can be a nonlinear object, and in this case, A would be parallel to the boundary of B, which is facing A. The same idea is also applicable for the parallelism between a *globally* aligned group of objects parallel to an object.

A. Parallelism With (Fuzzy) Linear Objects

Suppose that A is a linear object[4] and B is an object that is not necessarily linear. Both objects may be fuzzy. Let θ_A be the orientation of A and $\vec{u}_{\theta_A+(\pi/2)}$ be the normal unit vector to the principal axis of A. Then, according to the considerations of the introduction of this section, the relation "A is parallel to B" depends on two conditions.

1) There should be a large proportion of A that sees B in the direction $\vec{u}_{\theta_A+(\pi/2)}$.
2) The orientation of A and the orientation of the boundary of B that is facing A and that is seen by A in the direction $\vec{u}_{\theta_A+(\pi/2)}$ should be similar.

Both conditions deal with the notion of visibility. We model this notion using the directional dilation (9). Let Y be a fuzzy object with membership function μ_Y not intersecting X. We denote, by $X_{\mathrm{vis}(Y,\theta)}$, the subset of X that is seen by the points on the boundary of Y, i.e., the subset of X that is seen by Y, in the direction $\vec{u}_\theta$, and it is defined by

$$\mu_{X\,\mathrm{vis}(Y,\theta)}(x) = \mu_X(x) \wedge D_{\nu_\theta}(\mu_Y)(x) \tag{11}$$

where $D_{\nu_\theta}(\mu_Y)(x)$ is the directional dilation of μ_Y in the direction $\vec{u}_\theta$ [see (9)]. This definition is shown in Fig. 13. When A and B are linear segments, $A_{\mathrm{vis}(B,\theta_A+(\pi/2))}$ can be interpreted as the projection of B onto A.

For the first condition of parallelism, we are interested in the proportion of A that sees B in the direction $\vec{u}_{\theta_A+(\pi/2)}$.

[4]We consider that an object is linear if the ratio of its principal axis given by $(c_{yy} + c_{xx} - \sqrt{(c_{xx} + c_{yy})^2 - 4(c_{xx}c_{yy} - c_{xy}^2)})/(c_{yy} + c_{xx} + \sqrt{(c_{xx} + c_{yy})^2 - 4(c_{xx}c_{yy} - c_{xy}^2)})$, where $C = \begin{pmatrix} c_{xx} & c_{xy} \\ c_{yx} & c_{yy} \end{pmatrix}$ corresponds to the second moments matrix, is high [44].

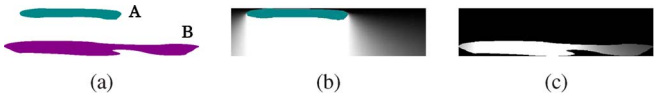

Fig. 13. Illustration of the notion of visibility for the objects A and B of (a). (b) Directional dilation $D_{\nu\theta_A+(\pi/2)}(A)$, which represents the visual field of A in the direction of $\theta_A+(\pi/2)$, where θ_A is the orientation of A (the white pixels have a high membership value of being observed by A in the direction $\theta_A+(\pi/2)$). (c) Membership function of $B_{\mathrm{vis}(A,\theta_A+(\pi/2))}$; the white pixels are the points with a high membership value.

The subset of A that sees B in the direction $\vec{u}_{\theta_A+(\pi/2)}$ is $A_{\mathrm{vis}(B,\theta_A-(\pi/2))}$. To measure this proportion, we make use of the fuzzy hypervolume V_n of a fuzzy set μ given by $V_n(\mu)=\sum_{x\in\mathfrak{I}}\mu(x)$ [1]. Hence, the proportion is equal to $V_n(\mu_{A\mathrm{vis}(B,\theta_A-(\pi/2))})/V_n(\mu_A)$.

For the second condition, we are interested only in the subset of the boundary of B that faces A and that is seen by the boundary of A in the direction θ_A. The boundary of B which faces an object A corresponds to the points on the boundary of B that delimit the region between A and B and are defined as the extremities of the admissible segments [45]. These are the points $b\in B$ for which there exists a point $a\in A$ such that the segment $]a,b[$ is included in $A^C\cap B^C$. In the case where A and B are fuzzy objects, we consider a fuzzy extension of this definition, and the degree of admissibility $\mu_{\mathrm{adm}}(b)$ is then defined as [45]

$$\mu_{\mathrm{adm}}(b)=\sup_{a\in\mathrm{Supp}(A)}\inf_{p\in]a,b[}\min\left(1-\mu_A(p),1-\mu_B(p)\right)$$

for $b\in\mathrm{Supp}(B)$, where $\mathrm{Supp}(B)$ is the support of μ_B, i.e., $\mathrm{Supp}(B)=\{x\in\mathfrak{I}|\mu_B(x)>0\}$, and $\mu_{\mathrm{adm}}(b)=0$ for $b\notin\mathrm{Supp}(B)$.

Therefore, the subset of the boundary of B that faces A and that is seen by the boundary of A in the direction $\theta_A+(\pi/2)$ is a fuzzy subset with the membership for a point $x\in\mathfrak{I}$ equal to the conjunction of its membership to B, the degree of being the extremity of an admissible segment and the degree of being seen by A. We denote this subset by $\delta B_{\mathrm{vis}(A,\theta_A+(\pi/2))}$ and its membership function by $\mu_{\delta B\mathrm{vis}(A,\theta_A+(\pi/2))}$

$$\mu_{\delta B\mathrm{vis}\left(A,\theta_A+\frac{\pi}{2}\right)}(x)=\mu_{\mathrm{adm}}(x)\wedge\mu_{B\mathrm{vis}\left(A,\theta_A+\frac{\pi}{2}\right)}(x)\quad(12)$$

where μ_{adm} represents the degree of being the extremity of an admissible segment.

Definition 4.1: The relation "A is parallel to B" is given by the following measure:

$$\mu_{\parallel}(A,B)=\frac{V_n\left(\mu_{A\mathrm{vis}\left(B,\theta_A-\frac{\pi}{2}\right)}\right)}{V_n(\mu_A)}\bigwedge\nu_0\left(\theta_{\delta B\mathrm{vis}\left(A,\theta_A+\frac{\pi}{2}\right)}-\theta_A\right)\quad(13)$$

where $\nu_0(\theta)$ is a trapeze membership function as the one in Fig. 2(b), which evaluates the degree to which $\theta_{\delta B\mathrm{vis}(A,\theta_A+(\pi/2))}$, the normal angle to $\delta B_{\mathrm{vis}(A,\theta_A+(\pi/2))}$ (computed as the direction orthogonal to the main orientation of δB_{vis}), and θ_A are "approximately" equal.

The relation defined by Definition 4.1 is invariant with respect to geometric transformations (translation, rotation, and scaling). It is not transitive, as discussed previously. However, we have a partial result in the crisp case. Suppose that A, B, and C are linear crisp segments, if $\mu_{\parallel}(A,B)=1$, $\mu_{\parallel}(B,C)=1$, and $\theta_A=\theta_B=\theta_C$, then $\mu_{\parallel}(A,C)=1$. This result shows that, in the crisp case, we have transitivity. To have the transitivity property, it is necessary that $\theta_A=\theta_B=\theta_C$, since $\nu_0(\theta_A-\theta_B)=1$ and $\nu_0(\theta_B-\theta_C)=1$ do not imply $\nu_0(\theta_A-\theta_C)=1$ due to the tolerance value t_1 of the function ν_0 [see Fig. 2(b)]. To have the transitivity without imposing the condition $\theta_A=\theta_B=\theta_C$, it is necessary that ν_0 is a linear function (i.e., $t_1=0$); however, this is restrictive.

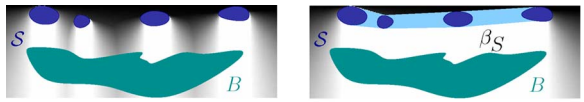

Fig. 14. (a) Visibility field of the group of objects $\mathcal{S}$. (b) Visibility field of the region between two consecutive members of (light blue) the group β_S and the group $\mathcal{S}$.

It is clear that the relation is reflexive. However, depending on the context, we may not want to consider intersecting objects as parallel. Thus, we can combine, in a conjunctive way, the previous degree (Definition 4.1) with a degree of nonintersection between the two sets.

B. Parallelism With a Globally Aligned Group of Objects

When considering parallelism with a *globally* aligned group of objects, the group has a similar role as the linear object in Definition 4.1. However, the visibility constraint should be computed in a modified way, discussed in the following.

Let $\mathcal{S}=\{A_0,\ldots,A_N\}$ be a *globally* aligned group, and let B be another object. The relation "$\mathcal{S}$ is parallel to B" has a high degree of satisfaction if there is a large portion of $\mathcal{S}$ that sees B, and this is computed in the same way as for the case of parallelism between a linear object and an object. For the second condition, we need to create the fuzzy set β_S which is composed of the union of the regions between two consecutive elements of $\mathcal{S}$. β_S can be constructed using the definition that involves the convex hull presented in [45]. In Fig. 14(b), an example of the region β_S of a group $\mathcal{S}$ is shown in light blue. From Fig. 14(a), we can see that the boundary of B that faces $\mathcal{S}$ and that is visible by $\mathcal{S}$ depends on the separation between the members of the group. However, it is desirable that the degree of parallelism of a group to an object is independent of this separation, because, if we add more elements to a group without changing its orientation or its extension, the degree of alignment to the object should remain the same. Therefore, in order to have a degree of parallelism independent of the separation of the members of the group, we use β_S in the second condition of parallelism. As for the definition of parallelism between objects, we combine the two conditions in a conjunctive way.

Definition 4.2: The degree of satisfaction of the relation "$\mathcal{S}$ is parallel to B" is given by

$$\mu_{\parallel}(\mathcal{S},B)=\frac{V_n\left(\vee_i\mu_{A_i\mathrm{vis}\left(B,\theta_s-\frac{\pi}{2}\right)}\right)}{V_n\left(\vee_i\mu_{A_i}\right)}\bigwedge\nu_0\left(\theta_{\delta B\mathrm{vis}\left(\beta_s\cup\mathcal{S},\theta_s+\frac{\pi}{2}\right)}-\theta_S\right)\quad(14)$$

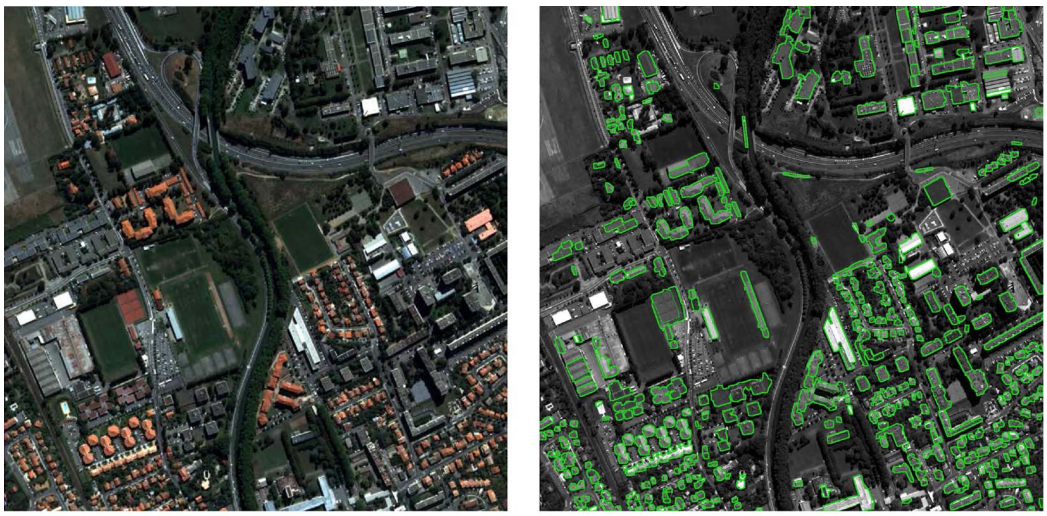

(a) (b)

Fig. 15. (a) Quickbird image of Toulouse, France. (b) Segmented buildings.

where θ_s is the orientation of the alignment of the group $\mathcal{S}$, as defined in Section III-F.

Using the same notations earlier, suppose that B is a fuzzy linear object. The degree of satisfaction of the relation "B is parallel to $\mathcal{S}$" is high if the orientation of B is similar to the orientation of the alignment of $\mathcal{S}$ and if there is a large proportion of B that sees the group of objects or β_S. As in Definition 4.2, it is necessary to use $\mathcal{S} \cup \beta_S$ in order to assure that the parallel relation is independent of the separation of the elements of $\mathcal{S}$.

Definition 4.3: The degree of satisfaction of the relation "B is parallel to $\mathcal{S}$" is given by

$$\mu_{\parallel}(B,\mathcal{S}) = \frac{V_n\left(\mu_{B\text{vis}\left(\mathcal{S}\cup\beta_S,\theta_B-\frac{\pi}{2}\right)}\right)}{V_n(\mu_B)} \bigwedge \nu_0(\theta_S-\theta_B) \quad (15)$$

where θ_B is the orientation of B.

Combining Definition 4.3 and Definition 4.2, we can define when a *globally* aligned group $\mathcal{S}=\{A_0,\ldots,A_N\}$ is parallel to another *globally* aligned group $\mathcal{T}=\{B_0,\ldots,B_M\}$.

Definition 4.4: The degree of satisfaction of the relation "$\mathcal{S}$ is parallel to $\mathcal{T}$" is given by

$$\mu_{\parallel}(\mathcal{S},\mathcal{T}) = \frac{V_n\left(\vee_i \mu_{A_i\text{vis}\left(\mathcal{T}\cup\beta_T,\theta_s-\frac{\pi}{2}\right)}\right)}{V_n\left(\vee_i \mu_{A_i}\right)} \bigwedge \nu_0(\theta_T-\theta_S) \quad (16)$$

where β_T is the region formed between two consecutive elements of $\mathcal{T}$ and θ_T is the orientation of alignment of the group $\mathcal{T}$.

Note that the quality of the segmentation is not critical to the evaluation of the parallel relation as soon as the general orientation of the object is well preserved.

V. Illustrative Examples

In this section, we present two examples to illustrate the possible applications of the proposed relations. For both examples, we used a Quickbird image of Toulouse, France, with a resolution of 0.6 m and size of 1420 × 1420 pixels, shown in Fig. 15(a).[5]

In the first example, we show how, by applying the alignment relation conjointly with the parallel relation between groups of aligned objects, it is possible to determine the residential areas composed of organized houses. For this, we first extracted the buildings by using the method described in [34], which found 2521 buildings. The results of the buildings segmentation are shown in Fig. 15(b). Note that the segmentation provides a very good localization of the buildings; however, there are some buildings which are divided into several regions and some others which have been fusioned. Therefore, we worked with a segmentation which was not perfect. In this example, we applied the method for determining the *global* alignments on the segmented buildings of Fig. 15. To determine the *globally* aligned groups of buildings, we used $\beta = 0.85$ and a Voronoï neighborhood constrained by a distance of 30 pixels equivalent to approximately 21 m and parameters $t_1 = 0.071$ rad and $t_2 = 0.095$ rad to construct the structuring element of the similarity relation of (6).

In the following, we explain how these parameters were chosen. In this example, we looked for groups of aligned buildings in residential areas which are strict alignments; thus, according to Section III-E, the degree of alignment should be larger than 0.8. Therefore, we applied the algorithm in Fig. 7 with increasing values of β from 0.85 to 1.0 in order to obtain all *locally* aligned groups with a degree larger than 0.85. Then, from these groups, we obtained the *globally* aligned groups with a degree greater than 0.85. The initial value of β is chosen according to the flexibility of the aligned groups that we want; however, if we are not sure how strict the alignments should be, then it is possible to choose a lower value of β. Using a lower value of β will increase the number of *globally* aligned groups. For the neighborhood, we chose a Voronoï neighborhood constrained by a distance $d = 30$ pixels. We chose this type of neighborhood since it gives a good representation of proximity,

[5]The DigitalGlobe identification of the image is 000000128955_01_P001.

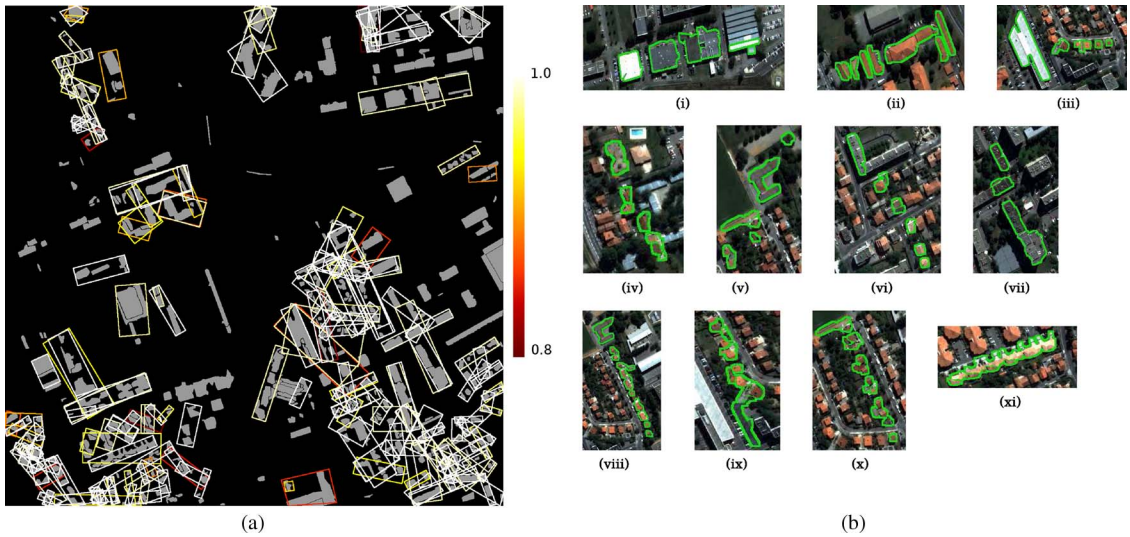

Fig. 16. (a) *Globally* aligned subsets of houses of Fig. 15 found by the algorithm with a degree of alignment larger than 0.85 using a Voronoï neighborhood constrained by 30 pixels. Each group is illustrated by a box around it; the color of the box represents the degree of alignment according to the color code shown by the bar on the right of the image. (b) Some examples of the *globally* aligned groups of (a).

and the parameter d is easily chosen as the maximum distance to which we tolerate buildings to be considered as neighbors in a residential area. This type of neighborhood has the advantage that it is based on the distribution of objects, and the distance parameter is used to avoid extreme cases, such as two objects which are very far away from each other but still considered as neighbors. This type of neighborhood can be used when the segmentation provides a good localization of the objects and there are not a lot of false alarms, since it only depends on the position of objects. Other neighborhoods, such as the one obtained when we consider all the objects which are at a distance inferior to d, can be used when there are a lot of false alarms. However, this second type of neighborhood has the disadvantage that it may be very sensitive to the choice of the parameter d. Another alternative is to use the fuzzy neighborhood which represents the notion of near (see Appendix), which, owing to the fuzzy representation, is less dependant on the choice of the parameters. Finally, the last parameters of the algorithm are the values t_1 and t_2 used to define the structuring element used for the dilation of the orientation histograms in the similarity measure in (6). These values are computed using (4) and (5). We set d_{average} to 15 pixels, which gives $t_1 = 0.071$ rad and $t_2 = 0.095$ rad. For d_{average}, we measure the distance between neighboring buildings in a small sample of the objects.

The resulting *globally* aligned groups of objects are shown in Fig. 16(a). In total, the algorithm found 233 groups. The computing time for this example was 5585 s in a computer with a processor Intel Core2 Duo of 2000 MHz and with 2 GB of RAM. This computation time could be significantly reduced by a careful code optimization.

In Fig. 16(b), we show some of these groups. We can see from Fig. 16(b)(i), (b)(iii), and (b)(viii) that the algorithm retrieved the groups even if they have objects of different sizes. The algorithm is also robust to segmentation errors: For instance, in Fig. 16(b)(ix), one of the buildings is merged with another region, and Fig. 16(b)(x) and (b)(xi) contains several buildings which are identified as one object. Moreover, all the groups shown in Fig. 16(b) are aligned even if the barycenters of the objects are not aligned. However, Fig. 16(b)(v) and (b)(vi) shows groups that do not give us any information to classify the buildings in a certain type of urban morphology, although they are aligned. This confirms again the importance of combining the alignment relation with the parallel relation.

Fig. 17. Clusters of houses belonging to *globally* aligned groups which are parallel and near to other groups with a degree greater than or equal to 0.8.

From the obtained *globally* aligned groups of houses, we extracted the groups which are parallel to another group or which have a group parallel to them and are close to another group to a degree larger than or equal to 0.8. The spatial relation "close to" was modeled in the same way as in [46]. For the parallel relation, we manually chose the parameters $t_1 = \pi/12$ and $t_2 = \pi/6$. These parameters correspond to the tolerance in considering that two angles are "approximately" the same. Although we chose these parameters manually, it is possible to learn them for a real application. The groups of houses satisfying the previous condition of parallelism are shown in Fig. 17. From the results, we can see that the regions containing

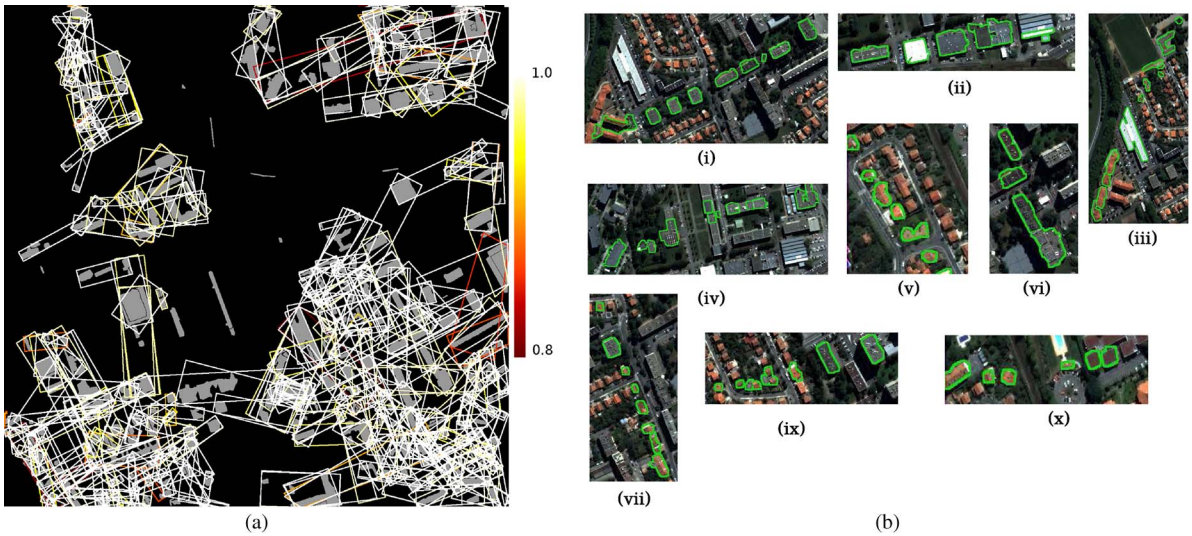

Fig. 18. (a) *Globally* aligned subsets of houses of Fig. 15 found by the algorithm with a degree of alignment larger than 0.85 using a Voronoï neighborhood constrained by 70 pixels. Each group is illustrated by a box around it; the color of the box represents the degree of alignment according to the color code represented by the bar on the right of the image. (b) Some examples of the *globally* aligned groups of (a).

organized groups of houses are well detected. This example shows how, by combining the two proposed spatial relations, it is possible to recognize a spatial urban pattern in the image.

The second example deals with false detections of roads near urban areas obtained from a road extractor [34]. Fig. 19(a) shows the result of this road detection algorithm. Some of the obtained roads are false detections. We know that, in residential areas, the houses are aligned and parallel to the roads. Therefore, in this example, we are mainly interested in determining the roads which have a group of buildings parallel to them. However, since some of the roads extracted in Fig. 19(a) consist of road's fragments, then we will be also interested in determining the roads which are parallel to a group of aligned buildings. As in the first example, we searched for strict alignments; therefore, we searched for the *globally* aligned groups with a degree larger than 0.85. We used again a Voronoï neighborhood constrained by a distance, but this time, the distance was equal to 70 pixels which is approximately 49 m. We changed the value of the distance because we are looking for long groups of aligned buildings in residential and industrial areas, and the distance between buildings in industrial areas is usually larger than that in residential areas. The parameters t_1 and t_2 of the similarity relation (6) are left unchanged.

The obtained results are shown in Fig. 18. We obtained a total of 478 groups. Some of the obtained groups are shown in detail in Fig. 18(b). All groups obtained in Fig. 16 are included or are part of a group of the ones obtained in Fig. 18. For example, the groups (ii), (iii), and (vi) of Fig. 18(b) contain the groups (i), (v), and (vii) of Fig. 16(b). From the results, we can see that we are able to extract very long groups of objects such as (i), (iii), (iv), and (vii) of Fig. 18(b); however, some of these groups do not represent meaningful alignments for the description of the scene. In the examples of Fig. 18(b), we can see that the method is able to extract groups containing objects of different sizes and whose barycenters are not necessarily aligned, even if the group can be considered as aligned.

To identify the false detections, we looked for the roads which were "close to" an aligned group of objects and which were parallel to a group or which had a group parallel to them. The identified roads are shown in Fig. 19(b) (we call this condition the constraint of parallelism). For the parallel relation, we used the parameters $t_1 = \pi/6$ and $t_2 = \pi/3$. These parameters were manually selected; however, they can be learned for a specific application.

Fig. 20 shows a region of the image containing the roads that satisfy the constraint of parallelism. We note that most of the roads which have a low degree of satisfaction of this constraint are the roads which can be classified as false detections. However, on the bottom of the image, we see three false detections that are still detected with a high degree. This is due to the fact that there are groups for which these roads are parallel. Based on the spatial relations, we have given a degree of satisfaction to the roads according to the relations, and this new information can be combined with other information, for instance, to find the roads which are "between" [45] groups of aligned buildings. All this information can be used to take a decision on whether or not the detected road is a false detection.

The two presented examples demonstrate the need of modeling the alignment relation considering each object as a whole, rather than only its center of mass. In these examples, we also show how to set the parameters of the presented methods.

The algorithms used to determine the degrees of satisfaction of the proposed relations are available at http://perso.telecom-paristech.fr/~bloch/tii/AlignmentParallelism.html, and the code compiles with Orfeo ToolBox [47] (http://www.orfeo-toolbox.org).

VI. Conclusion

After having highlighted the importance of alignment and parallelism for high-resolution remote sensing image interpretation, we have proposed fuzzy models for determining what is the degree of satisfaction of these relations in a set of objects in an image. The proposed models take into account

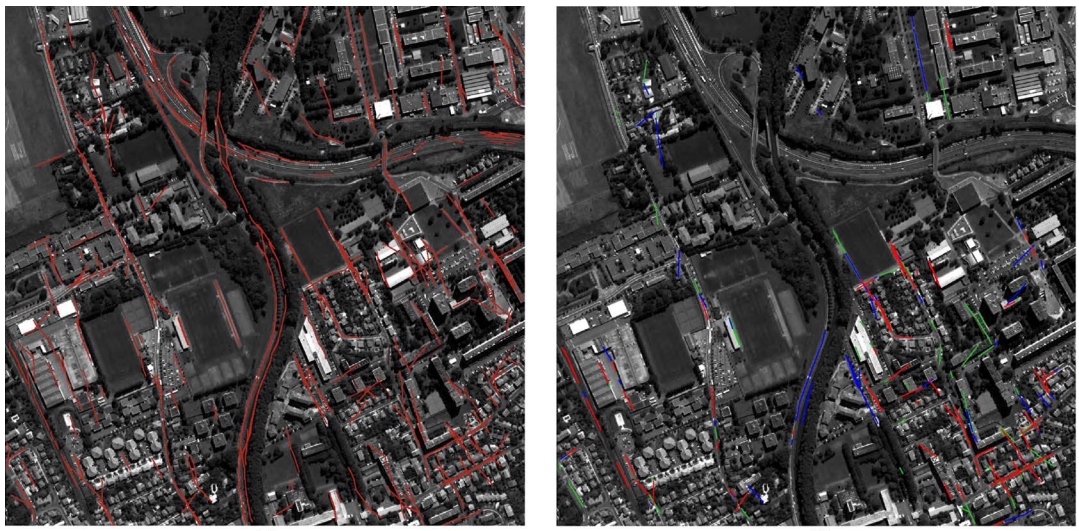

(a) (b)

Fig. 19. (a) Original detected roads. (b) Obtained roads, after eliminating the roads which are not parallel to a group or do not have a group parallel to them. The green, blue, and red roads represent the roads which satisfy the constraint of parallelism with a degree between 0.3 and 0.5, between 0.5 and 0.8, and between 0.8 and 1.0, respectively.

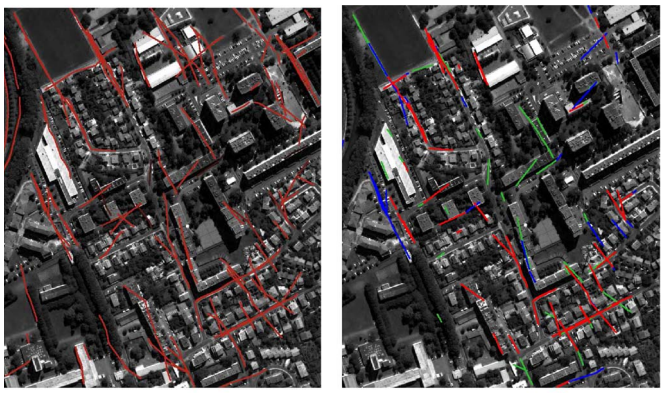

(a) (b)

Fig. 20. (a) Original roads of a subregion of Fig. 18(a). (b) Obtained roads, after eliminating the roads which were not parallel to a group or did not have a group parallel to them. The green, blue, and red roads represent the roads which satisfy the constraint of parallelism with a degree between 0.3 and 0.5, between 0.5 and 0.8, and between 0.8 and 1.0, respectively.

the semantic meaning of the relations. Two original definitions were presented for the alignment relation: *local* and *global* alignments. An algorithm for extracting *locally* aligned groups of objects was proposed, based on fuzzy relative position measures, which takes into account the imprecision inherent to the images and to the segmentation process. Based on the extraction of *locally* aligned groups of objects, we proposed a method for extracting *globally* aligned groups of objects using a graph-based approach. One of the advantages of the proposed fuzzy definitions is that the notion of alignment is a matter of degree, which fits the intuition. In concrete applications, the user could then be involved in the loop and could interact with the system to tune threshold values according to his own expectation of what aligned groups of objects should be and how strict or flexible he his.

As the parallel relation and the alignment relation are frequently found together, we presented a model for determining when a linear object is parallel to an object, when a group of *globally* aligned objects is parallel to an object, and when a linear object is parallel to a group of objects. We showed how the proposed models and algorithms can be extended to the case of fuzzy objects or when using fuzzy neighborhoods for the alignment relations.

The examples, on real objects extracted from satellite images, have shown the usefulness and power of the proposed models for scene understanding. Moreover, they can be used as intermediary steps for extracting objects in images. Other potential applications are classification and retrieval, as proposed, for instance, in [48].

Appendix
Other Neighborhood Choices in the Alignment Definition and Fuzzy Case

We can use other neighborhoods $N(A)$ for an object A in the alignment definitions. For instance, we can consider the neighborhood of objects that are "near" A which can be defined by the fuzzy morphological dilation $D^d_\nu(A)$ of A [49], where ν^d is a fuzzy structuring element representing the notion of a distance "less than" d. For a fixed ν^d, the neighborhood $N(A)$ is univocally defined. This choice gives a more restrictive condition of *local* alignment than using a Voronoï neighborhood, since the neighborhood contains more objects that should verify the alignment conditions. Moreover, it can also be used when A and B are fuzzy objects. In the following, we suppose that A and B are fuzzy objects defined through their membership functions μ_A and μ_B.

When considering a fuzzy neighborhood, the *Neigh* relation becomes also fuzzy, and we denote, by $\mu_{\mathrm{Neigh}}(A,B)$, its degree of satisfaction. By using a formal translation of the neighborhood relation, we define $\mu_{\mathrm{Neigh}}(A,B)$ as

$$\mu_{\mathrm{Neigh}}(A,B) = \mu_{\neg\,\mathrm{int}}(\mu_A,\mu_B) \wedge \mu_{\mathrm{int}}\left(\mu_{N(A)},\mu_B\right) \wedge \mu_{\mathrm{int}}\left(\mu_{N(B)},\mu_A\right) \quad (17)$$

where μ_{int} and $\mu_{\neg\,\mathrm{int}}$ are the degrees of intersection and non-intersection, respectively [1]. To have a symmetrical relation,

as in the adjacency relation in [1], we consider the intersection between μ_A and $\mu_{N(B)}$ and between μ_B and $\mu_{N(A)}$. However, in the case where $N(A) = D^d_\nu(A)$ with ν_d symmetric, then $\mu_{\text{int}}(\mu_{N(A)}, \mu_B)$ and $\mu_{\text{int}}(\mu_{N(B)}, \mu_A)$ are equal, and therefore, it is only necessary to verify one of the two conditions.

Consequently, the relation "connected by *Neigh*" also becomes a fuzzy relation denoted by μ_{conn}. The degree of connectedness in a group $\mathcal{S}$ between two objects A and B in $\mathcal{S}$ is defined as in [50] by

$$\mu_{\text{conn}}(A,B) = \max_{p \in P_{ab}} \left[\min_{1 \le i \le l_p} \mu_{\text{Neigh}} \left(C^{(p)}_{i-1}, C^{(p)}_i \right) \right] \quad (18)$$

where p is a list of objects $\langle C^{(p)}_0 = A, C^{(p)}_1, \ldots, C^{(p)}_{l_p} = B \rangle$ in $\mathcal{S}$, called path, and P_{ab} is the set of all the paths from A to B in $\mathcal{S}$. The degree of connectedness of a group can be defined as the minimum degree of connectedness between its elements

$$\mu_{\text{conn}}(\mathcal{S}) = \min_{A,B \in \mathcal{S}} \mu_{\text{conn}}(A,B). \quad (19)$$

When using a fuzzy neighborhood, the definitions of *globally* aligned and *locally* aligned have to be revised. The degree of *global* alignment of a group of objects $\mathcal{S} = \{A_0, \ldots, A_N\}$ and with $N \ge 3$ becomes

$$\mu_{\text{ALIG}}(\mathcal{S}) = \mu_{\text{conn}}(\mathcal{S}) \wedge \text{sim}\left(O\left(A_0, \mathcal{S} \setminus \{A_0\}\right), \ldots, O\left(A_N, \mathcal{S} \setminus \{A_N\}\right)\right). \quad (20)$$

This definition represents a conjunctive combination of the condition of being connected by the neighborhood relation and the similarity among the orientation histograms. When using a crisp neighborhood, this definition is equivalent to the one given in Definition 3.1, where the condition of satisfying the relation of connection by the neighborhood is implicit in the definition.

In a similar way, it is possible to extend the definition of *local* alignment to

$$\mu_{\text{LA}}(\mathcal{S}) = \mu_{\text{conn}}(\mathcal{S}) \wedge \left[\min_{X,Y,Z} \left(\text{sim}\left(O(X,Y), O(Y,Z)\right) \wedge \mu_{\text{conn}}\left(\{X,Y,Z\}\right) \right) \right]. \quad (21)$$

To identify the *locally* aligned groups, the edges of the neighborhood graph G_N are attributed with the degree of satisfaction of μ_{Neigh}. The notion of *triplets* also becomes fuzzy, and the degree to which three vertices X, Y, and Z form a *triplet* is given by the degree of connectedness of $\{X,Y,Z\}$ using (19). The construction of the dual graph considers the degree of connectedness, and only the *triplets* with a connectedness value greater than β are considered. Each edge (i,j) between the vertices $\tilde{V}_i$ and $\tilde{V}_j$ of the dual graph is attributed with the degree

$$\tilde{s}_{ij} = \text{sim}\left(O(X,Y), O(Y,Z)\right) \wedge \mu_{\text{conn}}\left(\{X,Y,Z\}\right) \quad (22)$$

where X,Y,Z is the *triplet* represented by the vertices $\tilde{V}_i$ and $\tilde{V}_j$. Finally, the *locally* aligned groups are obtained by applying algorithm in Fig. 7 on the dual graph. The choice of construction of the dual graph guarantees that the obtained groups satisfy (21).

ACKNOWLEDGMENT

The authors would like to thank V. Poulain for proving the segmentations of buildings and roads.

REFERENCES

[1] I. Bloch, "Fuzzy spatial relationships for image processing and interpretation: A review," *Image Vis. Comput.*, vol. 23, no. 2, pp. 89–110, Feb. 2005.

[2] S. Aksoy, C. Tusk, K. Koperski, and G. Marchisio, "Scene modeling and image mining with a visual grammar," in *Frontiers of Remote Sensing Information Processing*, C. Chen, Ed. Singapore: World Scientific, 2003, pp. 35–62.

[3] I. Bloch, T. Géraud, and H. Maître, "Representation and fusion of heterogeneous fuzzy information in the 3D space for model-based structural recognition—Application to 3D brain imaging," *Artif. Intell.*, vol. 148, no. 1/2, pp. 141–175, Aug. 2003.

[4] O. Colliot, O. Camara, and I. Bloch, "Integration of fuzzy spatial relations in deformable models—Application to brain MRI segmentation," *Pattern Recognit.*, vol. 39, no. 8, pp. 1401–1414, Aug. 2006.

[5] J. Keller and X. Wang, "A fuzzy rule-based approach to scene description involving spatial relationships," *Comput. Vis. Image Understand.*, vol. 80, no. 1, pp. 21–41, Oct. 2000.

[6] D. Guo, H. Xiong, V. Atluri, and N. Adam, "Object discovery in high-resolution remote sensing images: A semantic perspective," *Knowl. Inf. Syst.*, vol. 19, no. 2, pp. 211–233, May 2009.

[7] J. Mota, G. Câmara, M. Escada, O. Bittencourt, L. Fonseca, and L. Vinhas, "Case-based reasoning for eliciting the evolution of geospatial objects," in *Proc. 9th Int. COSIT*, 2009, pp. 405–420.

[8] F. L. Ber and A. Napoli, "Object-based representation and classification of spatial structures and relations," in *Proc. 14th IEEE ICTAI*, 2002, pp. 268–275.

[9] J. Inglada and J. Michel, "Qualitative spatial reasoning for high resolution remote sensing image analysis," *IEEE Trans. Geosci. Remote Sens.*, vol. 47, no. 2, pp. 599–612, Feb. 2009.

[10] A. Deruyver, Y. Hodé, and L. Brun, "Image interpretation with a conceptual graph: Labeling over-segmented images and detection of unexpected objects," *Artif. Intell.*, vol. 173, no. 14, pp. 1245–1265, Sep. 2009.

[11] J. Metzger, F. L. Ber, and A. Napoli, "Modeling and representing structures for analyzing spatial organization in agronomy," in *Proc. 11th ICCS*, Dresden, Germany, 2003, pp. 215–228.

[12] S. Steiniger and R. Weibel, "Relations among map objects in cartographic generalization," *Cartogr. Geograph. Inf. Sci.*, vol. 34, no. 3, pp. 175–197, Jul. 2007.

[13] M.-C. Vanegas, I. Bloch, H. Maître, and J. Inglada, "Approximate parallelism between fuzzy objects: Some definitions," in *Proc. WILF*, Palermo, Italy, 2009, vol. 5571, pp. 12–19.

[14] M.-C. Vanegas, I. Bloch, and J. Inglada, "Searching aligned groups of objects with fuzzy criteria," in *Proc. Int. Conf. IPMU*, Dortmund, Germany, 2010, pp. 605–613.

[15] M.-C. Vanegas, I. Bloch, and J. Inglada, "Detection of aligned objects for high resolution image understanding," in *Proc. IEEE IGARSS*, Honolulu, HI, 2010, pp. 464–467.

[16] D. G. Lowe, "Three-dimensional object recognition from single two-dimensional images," *Artif. Intell.*, vol. 31, no. 3, pp. 355–395, Mar. 1987.

[17] R. Mohan and R. Nevatia, "Using perceptual organization to extract 3D structures," *IEEE Trans. Pattern Anal. Mach. Intell.*, vol. 11, no. 11, pp. 1121–1139, Nov. 1989.

[18] R. Mohan and R. Nevatia, "Perceptual organization for scene segmentation and description," *IEEE Trans. Pattern Anal. Mach. Intell.*, vol. 14, no. 6, pp. 616–635, Jun. 1992.

[19] H.-B. Kang and E. Walker, "Perceptual grouping based on fuzzy sets," in *Proc. IEEE Int. Conf. Fuzzy Syst.*, 1992, pp. 651–659.

[20] J. Rouco, M. Penas, M. Penedo, M. Ortega, and C. Alonso-Montes, "Artificial intelligence techniques and recognition-certainty measure of pairwise line segment perceptual relations using fuzzy logic," in *Proc. Iberoamerican Congr. Pattern Recognit.*, 2007, pp. 477–486.

[21] A. L. Ralescu and J. G. Shanahan, "Perceptual organization for inferring object boundaries in an image," *Pattern Recognit.*, vol. 32, no. 11, pp. 1923–1933, Nov. 1999.

[22] S. Sarkar and K. L. Boyer, "Perceptual organization in computer vision: A review and a proposal for a classificatory structure," *IEEE Trans. Syst., Man, Cybern.*, vol. SMC-23, no. 2, pp. 382–399, Mar./Apr. 1993.

[23] A. Desolneux, L. Moisan, and J. M. Morel, *From Gestalt Theory to Image Analysis: A Probabilistic Approach*, vol. 34. New York: Springer-Verlag, 2008, ser. Interdisciplinary Applied Mathematics.
[24] M. Ortner, X. Descombes, and J. Zerubia, "Building outline extraction from digital elevation models using marked point processes," *Int. J. Comput. Vis.*, vol. 72, no. 2, pp. 107–132, Apr. 2007.
[25] M. Wertheimer, "Laws of organization in perceptual forms," in *Source Book of Gestalt Psychology*, W. H. Ellis, Ed. London, U.K.: Routledge and Kegan Paul, 1938.
[26] K. Koffka, *Principles of Gestalt Psychology*. New York: Harcourt Brace Jovanovich, 1935.
[27] L. Likforman-Sulem, A. Hanimyan, and C. Faure, "Extracting lines on handwritten documents by perceptual grouping," in *Proc. 3rd ICDAR*, 1995, vol. 2, pp. 774–777.
[28] H. Akcay and S. Aksoy, "Detection of compound structures using hierarchical clustering of statistical and structural features," in *Proc. IEEE IGARSS*, 2011, pp. 2385–2388.
[29] H. Kang and E. Walker, "Characterizing and controlling approximation in hierarchical perceptual grouping," *Fuzzy Sets Syst.*, vol. 65, no. 2/3, pp. 187–223, Aug. 1994.
[30] S. Christophe and A. Ruas, "Detecting building alignments for generalisation purposes," in *Proc. 10th Int. Symp. Spatial Data Handl. Adv. Spatial Data Handl.*, 2002, pp. 419–432.
[31] S. Toh, "Extracting viewpoint invariance relations using fuzzy sets," in *Proc. Intell. Veh. Symp.*, 1992, pp. 325–329.
[32] M. Pesaresi and J. Benediktsson, "A new approach for the morphological segmentation of high resolution satellite imagery," *IEEE Trans. Geosci. Remote Sens.*, vol. 39, no. 2, pp. 309–320, Feb. 2001.
[33] D. Comaniciu and P. Meer, "Mean shift analysis and applications," in *Proc. 7th IEEE ICCV*, Los Alamitos, CA, 1999, vol. II, pp. 1197–1203.
[34] V. Poulain, J. Inglada, M. Spigai, J. Tourneret, and P. Marthon, "High-resolution optical and SAR image fusion for building database updating," *IEEE Trans. Geosci. Remote Sens.*, vol. 49, no. 8, pp. 2900–2910, Aug. 2011.
[35] H. Sportouche, F. Tupin, and L. Denise, "Extraction and three-dimensional reconstruction of isolated buildings in urban scenes from high-resolution optical and SAR spaceborne images," *IEEE Trans. Geosci. Remote Sens.*, vol. 49, no. 10, pp. 3932–3946, Oct. 2011.
[36] E. Christophe and J. Inglada, "Robust road extraction for high resolution satellite images," in *Proc. IEEE ICIP*, San Antonio, TX, 2007, pp. V-437–V-440.
[37] K. Miyajima and A. Ralescu, "Spatial organization in 2D segmented images: Representation and recognition of primitive spatial relations," *Fuzzy Sets Syst.*, vol. 65, no. 2/3, pp. 225–236, Aug. 1994.
[38] D. Dubois and H. Prade, *Fuzzy Sets and Systems: Theory and Applications*, vol. 144. New York: Academic, 1980, ser. Mathematics in Science and Engineering.
[39] R. Zwick, E. Carlstein, and D. V. Budescu, "Measures of similarity among fuzzy concepts: A comparative analysis," *Int. J. Approx. Reason.*, vol. 1, pp. 221–242, 1987.
[40] I. Bloch, "On fuzzy distances and their use in image processing under imprecision," *Pattern Recognit.*, vol. 32, no. 11, pp. 1873–1895, Nov. 1999.
[41] J. Rabin, J. Delon, and Y. Gousseau, "Circular earth mover's distance for the comparison of local features," in *Proc. ICPR*, 2008, pp. 1–4.
[42] I. Bloch, C. Pellot, F. Sureda, and A. Herment, "Fuzzy modelling and fuzzy mathematical morphology applied to 3D reconstruction of blood vessels by multi-modality data fusion," in *Fuzzy Set Methods in Information Engineering: A Guided Tour of Applications*, R. Yager, D. Dubois, and H. Prade, Eds. New-York: Wiley, 1996, ch. 5, pp. 93–110.
[43] I. Bloch, "Fuzzy relative position between objects in image processing: A morphological approach," *IEEE Trans. Pattern Anal. Mach. Intell.*, vol. 21, no. 7, pp. 657–664, Jul. 1999.
[44] M. Peura and J. Iivarinen, "Efficiency of simple shape descriptors," in *Proc. 3rd Int. Workshop Vis. Form*, 1997, pp. 443–451.
[45] I. Bloch, O. Colliot, and R. Cesar, "On the ternary spatial relation between," *IEEE Trans. Syst., Man, Cybern. B, Cybern.*, vol. 36, no. 2, pp. 312–327, Apr. 2006.
[46] C. Hudelot, J. Atif, and I. Bloch, "Fuzzy spatial relation ontology for image interpretation," *Fuzzy Sets Syst.*, vol. 159, no. 15, pp. 1929–1951, Aug. 2008.
[47] J. Inglada and E. Christophe, "The Orfeo Toolbox remote sensing image processing software," in *Proc. IEEE IGARSS*, 2009, vol. 4, pp. IV-733–IV-736.
[48] S. Aksoy and R. Cinbis, "Image mining using directional spatial constraints," *IEEE Geosci. Remote Sens. Lett.*, vol. 7, no. 1, pp. 33–37, Jan. 2010.
[49] I. Bloch and H. Maître, "Fuzzy mathematical morphologies: A comparative study," *Pattern Recognit.*, vol. 28, no. 9, pp. 1341–1387, Sep. 1995.
[50] A. Rosenfeld, "Fuzzy digital topology," *Inf. Control*, vol. 40, no. 1, pp. 76–87, Jan. 1979.

Maria Carolina Vanegas received the B.S. degree in electronic engineering and mathematics from the Universidad de los Andes, Bogotá, Colombia, and the M.S. degree and the Ph.D. degree in image processing from Télécom ParisTech, Paris, France, in 2008 and 2011, respectively.

She is currently a Research Engineer with Carestream Dental, Croissy-Beaubourg, France. Her research interests include computer vision, image processing, spatial relations, and fuzzy sets in image processing.

Isabelle Bloch (M'94) received the B.S. degree from the Ecole des Mines de Paris, Paris, France, in 1986, the M.S. degree from the University Paris 12, Paris, in 1987, the Ph.D. degree from Ecole Nationale Supérieure des Télécommunications (Télécom ParisTech), Paris, in 1990, and the Habilitation degree from the University Paris 5, Paris, in 1995.

She is currently a Professor with the Signal and Image Processing Department, Télécom ParisTech, in charge of the Image Processing and Understanding Group. Her research interests include 3-D image and object processing; computer vision; 3-D and fuzzy mathematical morphology; information fusion; fuzzy set theory; structural, graph-based, and knowledge-based object recognition; spatial reasoning; and medical and satellite imaging.

Jordi Inglada (M'98) received the B.S. degree in telecommunications engineering from the Universitat Politècnica de Catalunya, Barcelona, Spain, in cooperation with the École Nationale Supérieure des Télécommunications de Bretagne, Brest, France, in 1997, and the Ph.D. degree in signal processing and telecommunications from the Université de Rennes 1, Rennes, France, in 2000.

He is currently with the Centre National d'Études Spatiales (French Space Agency), Toulouse, France, working in the field of remote sensing image processing with CESBIO. He is in charge of the development of image processing algorithms for the operational exploitation of Earth observation images, mainly in the field of multitemporal image analysis for land use and cover change.

Dr. Inglada is an Associate Editor of the IEEE TRANSACTIONS ON GEOSCIENCE AND REMOTE SENSING.